

**NEW TRANSFER FUNCTIONS FOR  
SIMULATION OF NATURALLY  
FRACTURED RESERVOIRS WITH  
DUAL POROSITY MODELS**

**A REPORT SUBMITTED TO THE DEPARTMENT OF PETROLEUM  
ENGINEERING**

**OF STANFORD UNIVERSITY**

**IN PARTIAL FULFILLMENT OF THE REQUIREMENTS FOR THE  
DEGREE OF MASTER OF SCIENCE**

**By  
Pallav Sarma  
May 2003**



I certify that I have read this report and that in my opinion it is fully adequate, in scope and in quality, as partial fulfillment of the degree of Master of Science in Petroleum Engineering.

---

Prof. Khalid Aziz  
(Principal Advisor)



## **Abstract**

The most popular and effective technique to model naturally fractured reservoirs has been through a dual porosity approach, where the fracture and matrix systems are separated into two different continuum, each with its own set of properties. They also interact with each other, i.e., fluid transfer takes place between them, governed by a transfer function. Most of the existing dual porosity models idealize matrix-fracture interaction by assuming orthogonal fracture systems (parallelepiped matrix blocks) and pseudo-steady state flow. This is rarely the case in real reservoirs. Further, the transfer function used to represent multiphase flow does not fully account for the main mechanisms governing multiphase flow. This work discusses techniques to remove many of these existing limitations in order to arrive at a transfer function more representative of real reservoirs.

Firstly, the mechanisms of single-phase mass transfer are discussed leading to a definition of the differential form of the transfer function. The limitations of current shape factors— a part of the transfer function— for single-phase flow are discussed. Combining the differential form of the single-phase transfer function and the single-phase pressure diffusion equation, an analytical form for a shape factor for transient pressure diffusion is derived. Further, a pseudo-steady shape factor for rhombic fracture systems is also derived. Finally, a general numerical technique to calculate the shape factor for any arbitrary shape of the matrix (i.e. non-orthogonal fractures) is proposed. This technique also accounts for both transient and pseudo-steady state pressure behavior. The results were verified against fine-grid single porosity models and were found to be in excellent agreement.

Secondly, mechanisms of two-phase mass transfer are discussed and a complete definition of the transfer function for two-phase/multiphase flow is derived. It is combined with flow governing equations for pressure and saturation diffusion to arrive at a modified form of the transfer function for two-phase flow that accurately takes into account pressure diffusion (fluid expansion) and saturation diffusion (imbibition), which are the

two main mechanisms driving multiphase flow. New shape factors for saturation diffusion are defined. Limitations of the current transfer function for multiphase flow are discussed, and it is shown that the prediction of wetting phase imbibition using the current transfer function is quite inaccurate, which might have significant consequences for reservoir management. Fine grid single porosity models are used again to verify the validity of the new transfer function. The results from single block dual porosity models and the corresponding single porosity fine grid models were in good agreement.

Thirdly, the proposed transfer function is extended for multiphase compositional flow, taking into account the effects of gravity segregation. The assumptions under which this extension is valid are also discussed.

Fourthly, a procedure to implement this complete dual porosity model into the General Purpose Research Simulator (GPRS) developed at Stanford is presented. The implementation's standard form is validated against the ECLIPSE 100 Dual Porosity Model and is found to be in perfect agreement.

## **Acknowledgments**

First and foremost, I would like to thank my adviser Dr. Khalid Aziz for his support, encouragement and guidance, and more so for always giving me enough independence to pursue my ideas. It is evident that this work would not have been possible without his patronage. I also wish to thank the rest of the Petroleum Engineering Department for their support and contributions to my academic achievements.

I am also very grateful to Dr. Fikri Kuchuk at Schlumberger for his invaluable comments and inspiration concerning my research.

Finally, I would like to thank the companies supporting the Reservoir Simulation Industrial Affiliate Program (SUPRI-B) at Stanford University for their financial contributions that made it this research possible.



# Contents

Abstract.....	v
Acknowledgments.....	vii
Contents .....	ix
List of Tables .....	xi
List of Figures .....	xiii
1 Introduction.....	1
1.1. Problem Definition.....	2
1.2. Outline.....	5
2 Literature Review.....	6
2.1. The Warren and Root Model .....	6
2.2. Extensions to Multiphase Flow.....	9
2.3. Further Modifications .....	12
2.4. The Current Transfer Function .....	20
2.5. Multiple Sub-domain Formulations.....	21
2.6. Summary .....	26
3 Single Phase Mass Transfer .....	27
3.1. Mechanisms of Mass Transfer .....	28
3.2. Single Phase Transfer Function .....	29
3.3. Limitations of Existing Models .....	30
3.4. Transient Pressure Behavior .....	34
3.5. Non-orthogonal Fracture Networks .....	37
3.6. A Generic Shape Factor Formulation .....	41
3.7. Validation and Comparison .....	45
4 Two Phase Mass Transfer .....	47
4.1. Mechanisms of Mass Transfer .....	47
4.2. The Two Phase Transfer Function .....	48
4.3. Limitations of Existing Models .....	50
4.4. Derivation of the Saturation Derivative .....	50
4.5. Derivation of the Pressure Derivative.....	55
4.6. Final Form of the Transfer Function.....	60
4.7. Validation and Comparison .....	62
5 Extensions to Three Phase Compositional Flow .....	69

6	Implementation into GPRS .....	71
6.1.	Modifications to Formulation .....	71
6.2.	Modifications to Design.....	79
6.3.	Validation of the Standard Model.....	84
7	Conclusions and Future Work .....	87
	Nomenclature .....	90
	References.....	92
A.	Shape Factor Software .....	95
B.	GPRS Dual Porosity Model .....	96

## List of Tables

<i>Table 2-1 Shape factor constant given by various researchers.....</i>	<i>19</i>
<i>Table 4-1 Properties of the validation model .....</i>	<i>63</i>
<i>Table 6-1 Properties of the test case reservoir.....</i>	<i>85</i>



## List of Figures

<i>Figure 1-1 Satellite image of the Circle Ridge Reservoir, Wyoming USA (www.fracturedreservoirs.com)</i> .....	1
<i>Figure 2-1 Idealization of the NFR system (Warren and Root, 1963)</i> .....	8
<i>Figure 2-2 The dual porosity model from a simulation perspective</i> .....	11
<i>Figure 2-3 Variation of transient shape factor with time</i> .....	19
<i>Figure 2-4 Dual porosity grid system with matrix subdomain decomposition (CMG, 2002)</i> .....	24
<i>Figure 2-5 Oil recovery and imbibition rate for rectangular matrix block (Wu and Pruess, 1986)</i> .....	26
<i>Figure 3-1 Conceptual representation of a fractured reservoir with sources and sinks</i> .....	29
<i>Figure 3-2 Cubic matrix with a single set of fractures (figure from Rangel-German, 2002)</i> .....	31
<i>Figure 3-3 Comparison of pressure drawdown of discrete fracture model and dual porosity models</i> .....	32
<i>Figure 3-4 A Rhombic matrix block</i> .....	33
<i>Figure 3-5 An equivalent square matrix block</i> .....	33
<i>Figure 3-6 Pressure response of rhombic and square matrix blocks</i> .....	34
<i>Figure 3-7 Matrix abstraction to model transient flow</i> .....	35
<i>Figure 3-8 Comparison of numerical and analytical pressure response for a cubic matrix block</i> .....	37
<i>Figure 3-9 The rhombic matrix abstraction</i> .....	38
<i>Figure 3-10 Pressure solution using Matlab PDE Toolbox</i> .....	42
<i>Figure 3-11 The shape factor for a rhombic matrix block calculated numerically</i> .....	43
<i>Figure 3-12 Comparison of 1D superposition and 2D solution</i> .....	44
<i>Figure 3-13 Comparison of discrete fracture model and dual porosity models with different shape factors</i> .....	45
<i>Figure 4-1 Conceptual representation of a fractured reservoir with sources and sinks</i> .....	48
<i>Figure 4-2 An arbitrary matrix block with fractures on all sides</i> .....	49
<i>Figure 4-3 Cubic matrix with two fractures, with imbibition through one fracture</i> .....	63
<i>Figure 4-4 Saturation profile at 20 days</i> .....	64

<i>Figure 4-5 Pressure profile at 1 day.....</i>	<i>64</i>
<i>Figure 4-6 Comparison of oil production rates for <math>m = 1.06</math> .....</i>	<i>66</i>
<i>Figure 4-7 Comparison of water imbibition rates for <math>m = 1.06</math>.....</i>	<i>67</i>
<i>Figure 4-8 Explanation of 0 initial imbibition rate for current transfer function.....</i>	<i>67</i>
<i>Figure 6-1 Structure of reservoir part of jacobian (Cao, 2002).....</i>	<i>74</i>
<i>Figure 6-2 New structure of jacobian.....</i>	<i>75</i>
<i>Figure 6-3 Simple NFR with two wells completed in fracture system.....</i>	<i>76</i>
<i>Figure 6-4 Structure of jacobian for the above reservoir.....</i>	<i>77</i>
<i>Figure 6-5 jacobian structure for Dual Porosity transfer derivatives .....</i>	<i>78</i>
<i>Figure 6-6 jacobian structure for 2-point flux derivatives .....</i>	<i>78</i>
<i>Figure 6-7 Domain level system model.....</i>	<i>80</i>
<i>Figure 6-8 Reservoir level system model (modified) .....</i>	<i>81</i>
<i>Figure 6-9 Modifies formulation level system model .....</i>	<i>83</i>
<i>Figure 6-10 Inheritance structure for the flow equation modules.....</i>	<i>83</i>
<i>Figure 6-11 Quarter five-spot test case.....</i>	<i>85</i>
<i>Figure 6-12 Producer well block pressure vs. time .....</i>	<i>86</i>
<i>Figure 6-13 Producer water cut vs. time .....</i>	<i>86</i>

# Chapter 1

## 1 Introduction

A naturally fractured reservoir (NFR) can be defined as a reservoir that contains fractures (planar discontinuities) created by natural processes like diastrophism and volume shrinkage, distributed as a consistent connected network throughout the reservoir (Ordonez et al., 2001). Fractured petroleum reservoirs represent over 20% of the world's oil and gas reserves (Saidi, 1983), but are however among the most complicated class of reservoirs to produce efficiently. A typical example is the Circle Ridge fractured reservoir located on the Wind River Reservation in Wyoming, USA. This reservoir has been in production for more than 50 years but the total oil recovery until now has been less than 15% ([www.fracturedreservoirs.com](http://www.fracturedreservoirs.com), 2000).

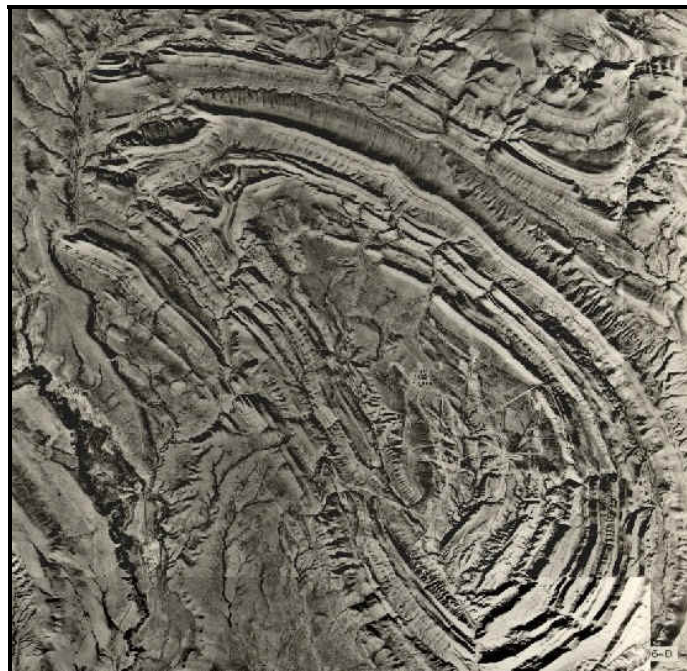


**Figure 1-1** Satellite image of the Circle Ridge Reservoir, Wyoming USA ([www.fracturedreservoirs.com](http://www.fracturedreservoirs.com))

It is undeniable that reservoir characterization, modeling and simulation of naturally fractured reservoirs present unique challenges that differentiate them from conventional, single porosity reservoirs. Not only do the intrinsic characteristics of the fractures, as well as the matrix, have to be characterized, but the interaction between matrix and fractures must also be modeled accurately. Further, most of the major NFRs have active aquifers associated with them, or would eventually resort to some kind of secondary recovery process such as waterflooding (German, 2002), implying that it is essential to have a good understanding of the physics of multiphase flow for such reservoirs. This complexity of naturally fractured reservoirs necessitates the need for their accurate representation from a modeling and simulation perspective, such that production and recovery from such reservoirs be maximized.

## **1.1. Problem Definition**

NFRs are usually thought to comprise of an interconnected fracture system that provides the main flow paths (they have high permeability and low storage volume), and the reservoir rock or matrix that acts as the main source of hydrocarbons (they have low permeability and high storage volume) (Beckner, 1990). Thus it is the matrix system that contains most of the oil, but the production of oil to the wells is through the high permeability fracture system, implying that it is the matrix-fracture interaction that mainly controls fluid flow. Production from the matrix-fracture system can be associated with various physical mechanisms including oil expansion or pressure diffusion, imbibition or saturation diffusion, gravity imbibition or drainage, mass diffusion and viscous displacement or convection (ECLIPSE 100 Technical Description, 2000). As will be seen later, the first two mechanisms are the predominant ones for most NFRs and the third is also important for certain reservoirs. The last two can be usually neglected, as their effect is insignificant compared to the others. We should note here that this is quite unlike single porosity reservoirs, where viscous displacement caused by source/sink pressure gradients is the main mass transfer mechanism.

### ***1.1.1. Challenges in NFR Simulation***

As mentioned before, NFRs present many unique and complex challenges from a modeling and simulation perspective. This is primarily because of the combined effect of the coexistence of two very different kinds of media from a fluid flow standpoint, and complex interaction of the various mechanisms governing mass transfer. Multiphase flow in fractured reservoirs depends among other things upon the combined, nonlinear effects of hydraulic connectivity and wettability of fractures and matrix, rock-matrix permeability and porosity, matrix-block size and shape, capillary pressure, and the interfacial tension between the different phases (German, 2002). It is for these reasons that matrix-fracture transfer governed by these various interactions is not yet understood fully and therefore is a significant unknown in reservoir simulation of NFRs. And since the matrix-fracture interaction controls fluid flow, performance of any predictive model would be significantly impacted by how accurately this matrix-fracture transfer is modeled.

Another major cause of the complexity of modeling and simulating NFRs is due to the highly heterogeneous and anisotropic nature of the fracture system (Ordonez et al., 2001, He et al., 2001). The heterogeneity is a result of the complex spatial variation in the distribution and directionality of the fractures and also because the properties of the fracture system itself tends to vary spatially. For example, the width and the amount of cementing material in fractures that determine the permeability might vary significantly with location. Because of its highly heterogeneous nature, it is in general very difficult to accurately characterize the spatial distribution of the fracture system, which define the main flow paths of the reservoir. The anisotropy creeps in as a result of the extreme difference in the fluid flow properties of the matrix and fracture systems and also because of the highly directional nature of the fracture system. Inability to model these accurately will have a major impact on accurate predictions of the ultimate recovery from such reservoirs.

Yet another complexity arises from the nature of fracture-fluid interaction, which is modeled through fracture relative permeability and capillary pressure curves (German, 2002). These properties have a tremendous impact on the outcome of NFR simulation, but are inherently more difficult to determine as compared to the matrix-fluid interaction

properties. Even laboratory experiments fail to correctly determine these properties for the fracture system. Thus fracture-fluid interaction is still an active area of research.

### ***1.1.2. The Dual Porosity Model***

With currently existing computational capabilities, modeling typical massively fractured NFRs with conventional fine grid single porosity models would be quite impossible. This is due to the sheer number of grids that would be required to simulate matrix-fracture flow rigorously. And even if this was somehow possible, there is always the philosophical question of the necessity of accurate modeling to the pore or micro-fracture scale. Thus the traditional yet efficient and effective approach to model NFRs has been through a “Dual Porosity” model, where the fracture and matrix systems are separated into different continua, each with its own set of properties characteristic to the matrix and fracture systems. Matrix-fracture interaction governing mass transfer between matrices and fractures is modeled through a “Transfer Function” (Barenblatt, 1960). It is obvious that with this definition, the formulation for a dual porosity model would be very similar to a conventional single porosity model, except for the presence of the new transfer function. This transfer function is the heart of the dual porosity model as it controls matrix fracture interaction, which, as we saw is the main force that controls production performance of a NFR. The various existing formulations of the dual porosity model mainly differ in the manner this transfer function is defined.

The existing formulations of the dual porosity model have many limitations in the sense that they have been derived with many simplified and idealized assumptions, and particularly, is mathematically rigorous only for single-phase flow, as we will see later. This dissertation is an attempt to investigate matrix-fracture interaction –the first complexity of NFRs- modeled in the dual porosity abstraction through the transfer function, with the final objective of removing many of the existing limitations in order to arrive at a transfer function for multiphase flow more representative of real NFRs. It should however be understood at this point that a simulation model of any NFR would

only be representative if all the three causes of complexity mentioned before are recognized and modeled appropriately.

## **1.2. Outline**

This dissertation is organized in a manner that follows a gradual process of developing a conceptual and logical understanding of the basic dual porosity model and its limitations, and then progress through a mathematical and physical discussion of the mechanisms of matrix-fracture interaction culminating in a definition of a complete transfer function for multiphase flow and its implementation.

The second chapter is a review of existing dual porosity models and its extensions. The basic dual porosity formulation and its modifications will be discussed along with their limitations in order to motivate the need for an improved formulation from a mathematical and physical standpoint.

The third chapter discusses the limitations of the existing shapes factor for single-phase flow and proposes a general numerical technique to calculate the shape factor for any arbitrary shape of the matrix (i.e. non-orthogonal fractures). This technique also accounts for both transient and pseudo-steady state pressure behavior. The results were verified against fine-grid single porosity models and were found to be in excellent agreement.

In the fourth chapter, mechanisms of two-phase mass transfer are first discussed and a complete definition of the transfer function for two-phase flow is derived. Limitations of the current transfer function for multiphase flow are discussed, and advantages of the new transfer function are demonstrated. Fine grid single porosity models are used again to verify the validity of the new transfer function.

The fifth chapter discusses the extensions of the previously derived model for multiphase compositional flow, taking into account the effects of gravity segregation. The assumptions under which this extension is valid are also discussed.

The sixth chapter is a discussion of the procedure to implement this complete dual porosity model into the General Purpose Research Simulator (GPRS) developed at

Stanford. The implementation's standard form is validated against the ECLIPSE 100 Dual Porosity Model and is found to be in perfect agreement.

The final chapter is a conclusion of the results and insights obtained through this work regarding dual porosity models, wrapping up with a discussion of areas of future work in NFR simulation.

## **Chapter 2**

### **2 Literature Review**

The foundation of the dual porosity model was laid down by Barenblatt (1960) and Warren and Root (1963) more than forty years ago. The following era has seen many modifications to the basic dual porosity model by various researchers. This chapter discusses in detail many of the various formulations and extensions of the dual porosity model since Warren and Root's (1963) original publication along with their limitations, and motivates the need for an improved formulation.

#### **2.1. The Warren and Root Model**

Warren and Root (1963) proposed an analytic solution for single-phase unsteady-state, radial flow in a naturally fractured reservoir and introduced the dual porosity concept to petroleum engineering. Their formulation was primarily designed for application to well testing. Their double porosity domain assumes a continuous uniform fracture network oriented parallel to the principal axes of permeability. The matrix blocks in this system occupy the same physical space as the fracture network and are assumed to be identical rectangular parallelepipeds with no direct communication between matrix blocks. The matrix blocks are also assumed to be isotropic and homogeneous. Figure 2-1 demonstrates the idealization as proposed.

The mathematical model describing the above idealization leads to the continuity equation for a 2D fracture domain and a slightly compressible fluid was given as (Warren and Root, 1963):

$$\frac{k_{fx}}{\mu} \frac{\partial^2 p_f}{\partial x^2} + \frac{k_{fy}}{\mu} \frac{\partial^2 p_f}{\partial y^2} - \phi_m C_m \frac{\partial p_m}{\partial t} = \phi_f C_f \frac{\partial p_f}{\partial t} \quad (2.1)$$

Subscript  $f$  stands for fracture parameters and subscript  $m$  stands for matrix parameters. Here, the x-axis and the y-axis coincide with the principle axes of the permeability field. We observe that this is very similar to the continuity equation for a single porosity medium except for the presence of a source term given by the last term of the LHS. According to Warren and Root (1963), if pseudo-steady state exists in the matrix system, then Darcy's law is applicable and the following equation must be satisfied at each point within the matrix system:

$$\phi_m C_m \frac{\partial p_m}{\partial t} = \frac{\sigma k_m}{\mu} (p_f - p_m) \quad (2.2)$$

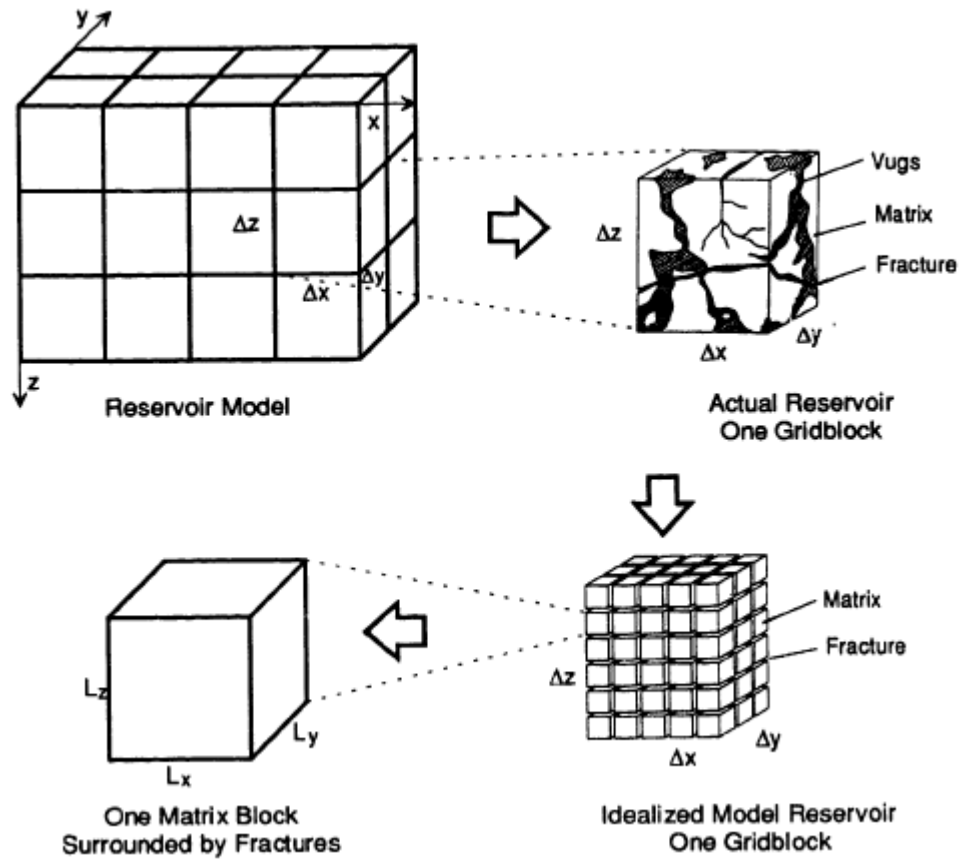


**Figure 2-1** Idealization of the NFR system (Warren and Root, 1963)

These two equations define the complete dual porosity model for a single-phase system. Warren and Root (1963) gave an analytical solution for the above system applicable to well testing. It is important to understand that the first equation is the equation governing fluid flow in the fracture system and the second for the matrix system. Equation 2.2 is also equal to the transfer function because it is assumed that there is no direct communication between matrix blocks, meaning that all fluid transfer in the matrix system is only between the fracture and matrices. The finite difference form of the above would give the simulator equations for a dual porosity single-phase system.

The parameter  $\sigma$  in Equation 2.2 has the dimensions of reciprocal area and is defined as a shape factor that reflects the geometry of the matrix elements and controls flow between the two porous media. Warren and Root (1963) gave the following definition of the shape factor for cubic matrix blocks:

$$\sigma = \frac{4n(n+2)}{l^2} \quad (2.3)$$

Here  $n$  is the set of normal fractures and  $l$  is a characteristic length given by the equations below where  $a$ ,  $b$  and  $c$  are lengths of the sides of a cubic matrix block. These equivalence relations are obtained using volume to surface ratios.

$$\begin{aligned} l &= \frac{3abc}{ab+bc+ca} & \in \mathbf{n} = 3 \\ l &= \frac{2ab}{a+b} & \in \mathbf{n} = 2 \\ l &= a & \in \mathbf{n} = 1 \end{aligned} \quad (2.4)$$

It should be understood here that the shape factor so defined is not completely rigorous mathematically, as its derivation does not utilize the pressure diffusion equation governing fluid flow within the matrix block, but uses an integral material balance combined with the assumption of pseudo-steady state flow.

## 2.2. Extensions to Multiphase Flow

The formulation of Warren and Root (1963) was extended directly for multiphase flow by Kazemi et al. (1976), and they solved the dual porosity system in three dimensions numerically. As with the Warren and Root model, two differential equations are required to define the complete system - one for flow in the fractures and another for flow in the matrix. The finite difference form of the differential flow equations for the fracture and matrix systems with immiscible black oil fluids are given as follows by Kazemi et al (1976):

$$\left\{ \sum_l T_l \lambda_p \rho_p \Delta (p_p - \gamma_p D) + \rho_p q_p^w \right\}_f - \tau_{mf} = \left\{ \frac{V}{\Delta t} \Delta_t (\phi S_p \rho_p) \right\}_f \quad (2.5)$$

$$\tau_{mf} = \left\{ \frac{V}{\Delta t} \Delta_t (\phi S_p \rho_p) \right\}_m \quad (2.6)$$

Subscript  $p$  stands for the two components (or phases, as the system is immiscible) oil and water. The transfer function  $\tau_{mf}$  is given as:

$$\tau_{mf} = k_m V \sigma \lambda_p \rho_p \left[ (p_p - \gamma_p D)_f - (p_p - \gamma_p D)_m \right] \quad (2.7)$$

Kazemi et al. gives the following definition for the shape factor:

$$\sigma = 4 \left[ \frac{1}{L_{mx}^2} + \frac{1}{L_{my}^2} + \frac{1}{L_{mz}^2} \right] \quad (2.8)$$

We observe that their shape factor is not the same as that obtained by Warren and Root (1963). This is because as mentioned before, Warren and Root (1963) uses the concept of a “characteristic length” and derives the shape factor based on an integral material balance on this length. They then relate this characteristic length to the sides of a cubic matrix block based on volume to surface ratios. Kazemi et al. (1976) derived their shape factor based on a direct material balance on a cubic matrix block under assumptions of pseudo-steady state.

However, there are other assumptions even more critical to the validity of the model. Firstly, we observe that this model is a direct generalization of the single-phase model given by Warren and Root (1963). The main mechanism governing matrix-fracture mass transfer for a single-phase system is fluid expansion. But for multiphase systems, we have two additional mechanisms, imbibition and gravity segregation, which might even be more important than fluid expansion. The direct generalization of including gravity by replacing pressure with potential in the transfer function has the inherent assumption than linear superposition of the two mechanisms is applicable. Further, imbibition is assumed to be taken care of by the use of capillary pressures as in single porosity flow without any physical basis for applicability to dual porosity systems.

In addition, there are a few other assumptions as well, but these are also true for single porosity systems. Since the matrix block is not discretized, block averaged values of potential, saturation, capillary pressure and relative permeability are used in their transfer function. This block averaged saturation is the same type of average saturation encountered in conventional, single porosity simulation. In single porosity simulation no saturation or pressure gradients can be resolved at a scale smaller than the computational gridblock. A similar uniform pressure and saturation distribution is assumed in a dual porosity formulation within the gridblock. However, an additional level of inaccuracy exists in a dual porosity model due to the fact that a gridblock in general would contain more than one matrix block. Therefore all the matrices within a gridblock have the same pressure and saturation. Thus, smaller the gridblocks better will be the accuracy, but it would also require greater computational power. This is a tradeoff that would always exist between the level of resolution and computational speed.

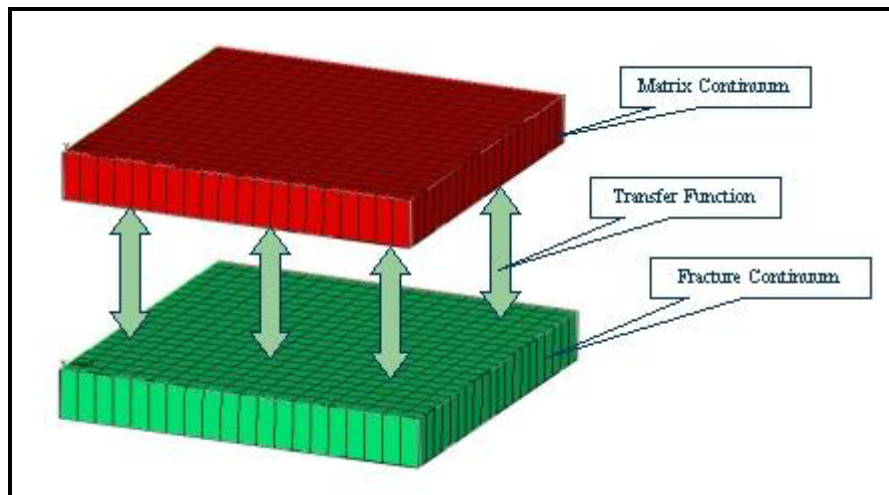


**Figure 2-2** The dual porosity model from a simulation perspective

Inspection of Equations 2.5 and 2.6 shows that this dual porosity formulation reduces to the standard black oil formulation if  $\tau_{mf} = 0$ . This offers a great advantage in the sense that simulating reservoirs with fractured and non-fractured regions or only single porosity reservoirs is possible with the same set of dual porosity Equations.

### 2.3. Further Modifications

Since its proposal, many researchers have made significant extensions to the dual porosity model of Kazemi et al. (1976) As mentioned before, modification of the original dual porosity formulation is necessary because the physics of multiphase flow found in naturally fractured systems is not adequately described by the direct generalization of single phase equations proposed by Warren and Root (1963).

Gilman and Kazemi (1983) updated the earlier dual porosity simulator of Kazemi et al. (1976) by modifying the treatment of mobility. They altered the matrix/fracture transfer function of Equation 2.7 to include fracture relative permeability when fluid is flowing from the fracture to the matrix. This updated matrix/fracture transfer term is:

$$\tau_{mf} = k_m V \sigma \left\{ \omega_p \lambda_{pm} + (1 - \omega_p) \lambda_{pf} \right\} \rho_p \left[ (p_p - \gamma_p D)_f - (p_p - \gamma_p D)_m \right] \quad (2.9)$$

They recognized that as saturation gradients within the matrix block cannot be resolved in the dual porosity model, upstream weighting might not be appropriate always (will be discussed in detail later). Here  $\omega_p$  is a weighting factor which varies from 0 to 1 and is equal to 1 if flow in from matrix to fracture. Further improvements to their simulator allowed Gilman and Kazemi (1983) to also account for matrix/fracture flow due to an imposed pressure gradient in the fracture. A dynamic gravity potential was used that was based on the potential of matrix subdomains and a fracture potential calculated at the same elevation as its corresponding matrix subdomain. By setting the relative permeability of the matrix subdomain equal to the fraction of subdomain face covered by water, they improved their imbibition modeling as only those matrix subdomains in contact with water could imbibe.

Thomas, Dixon and Pierson (1983) presented another version of a fully implicit, three-dimensional, multiphase naturally fractured simulator based on the dual porosity approach. Gravity effects in their transfer term were modeled through the use of pseudo-relative permeability and capillary pressure curves. A provision for matrix/fracture flow due to a pressure gradient in the fracture system was also included. The transfer due to an

imposed pressure gradient in the fracture across the matrix block was represented as an additional source term to the total matrix/fracture transfer term.

To simulate the matrix block boundary condition during imbibition the water relative permeability in their matrix/fracture transfer function was maintained at the  $k_{rw}$  value corresponding to the matrix water saturation at zero oil-water capillary pressure. They multiplied the matrix phase relative permeability values by the fracture phase saturations to include the effect of block coverage: i.e. not all matrix blocks within a computational cell will undergo imbibition when the fracture water level is positioned within the gridblock. So for water flowing from the fracture to the matrix the relative permeability in Equation 2.7:

$$k_{rw} = S_{wf} [k_{rw}]_{P_c=0} \quad (2.10)$$

And for oil flowing from the fracture to matrix system:

$$k_{ro} = S_{of} [k_{ro}]_{S_{wm}} \quad (2.11)$$

For flow from the matrix to the fracture unaltered matrix relative permeability values are used in the matrix/fracture transfer function. The matrix/fracture transfer term proposed by Thomas et al. (1983) is thus given by:

$$\tau_{mf} = k_m V \sigma \left\{ \omega_p \lambda_{pm} + (1 - \omega_p) \lambda_{pf}^* \right\} \rho_p \left[ (p_p - \gamma_p D)_f - (p_p - \gamma_p D)_m \right] \quad (2.12)$$

When flow is coming from the fractures,  $\omega_p = 0$  and the value of  $\lambda_{pf}^*$  is given based on  $k_r$  values given by Equations 2.11 and 2.12.

To test the validity of their formulation, fine grid simulations of imbibition in a single matrix block surrounded by fractures were made using a single porosity simulator. The matrix block was subjected to boundary conditions of complete immersion and they found that by varying the shape factor a good match between the dual porosity and single

porosity results could be obtained. However, the matching shape factor did not correspond to the actual size of the matrix block. Additionally, the dual porosity simulations required a different shape factor to match the fine grid results depending on whether the process was water imbibition in a water/oil system or gravity drainage in a gas/oil system. These observations suggest that the above formulations lack in generality, as the shape factor cannot be easily specified for any matrix/fracture system and further, it appears to be process dependent. In fact, the above two formulations also have a limitation due to the fact that the use of weighted average motilities is nonphysical. This is because, just like single porosity systems, saturation transport phenomenon is described by hyperbolic equations, and therefore is only dependent on upstream properties.

Litvak (1985) presented a dual porosity formulation with a modified gravity potential, which is based upon the fluid levels in the matrix and fracture and so changes with any fluid exchange between the fracture and matrix. His matrix/fracture transfer term is given as:

$$\tau_{mf} = k_m V \sigma \lambda_p \rho_p C_{pf} \left[ p_{pf} - p_{pm} - (\gamma_w - \gamma_o)(D_{pm} - D_{pf}) \right] \quad (2.13)$$

The gravity term in the above equation defines the gravity head with segregated water levels in the matrix and fracture. The  $C_{pf}$  multiplier is a coverage factor, not fully defined in the reference, that gives some connection between the matrix/fracture imbibition rate and the fracture water level. For a block suddenly immersed in water  $C_{pf} = 1$ . Such a block should have a larger imbibition transfer rate than a block immersed only partially in water for which  $C_{pf} < 1$ . From this it appears that  $C_{pf}$  should be proportional to the fracture water saturation (Beckner, 1990). The shape factor defined here is the same as that given by Kazemi et al. (1976), and therefore all limitations of the shape factor applicable to their formulation are also applicable here. There is also the question of proper boundary conditions on the matrix/fracture interface that is not addressed in the matrix/fracture transfer given by Equation 2.13. Differences in immersed versus moving or partially immersed boundary conditions are not considered.

Another dynamic gravity function presented by Sonier, Sonillard and Blaskovich (1986) assumes that the phase saturations within the fractures are the same in any portion of the grid cell and that all the matrix blocks within the grid cell have the same saturation. Their matrix/fracture transfer term has the same form as the transfer function of Gilman and Kiazemi (1983) except for different description of the gravity potential between the matrix and fracture. For an oil-water system their transfer term is defined as:

$$\tau_{mf} = k_m V \sigma \left\{ \omega_p \lambda_{pm} + (1 - \omega_p) \lambda_{pf} \right\} \rho_p \left[ (p_p - \gamma_p Z)_f - (p_p - \gamma_p Z)_m \right] \quad (2.14)$$

Here the water levels in the fracture and matrix are defined as:

$$Z_f = \frac{(S_{wf} - S_{iwf}) L_{mz}}{1 - S_{orf} - S_{iwf}} \quad (2.15)$$

$$Z_m = \frac{(S_{wm} - S_{iwm}) L_{mz}}{1 - S_{orm} - S_{iwm}}$$

$S_{iwf}$  and  $S_{iwm}$  are the initial water saturations in the fracture and matrix and  $S_{orf}$  and  $S_{orm}$  are the residual oil saturations in these two media. The use of phase densities instead of the density contrast is a shortcoming of this type of gravity modeling when compared to the Litvak (1985) formulation.

Rossen and Shen (1987) proposed a formulation that models the matrix/fracture transfer due to gravity and imbibition through the use of pseudo-capillary pressure curves for both the fracture and matrix. The matrix pseudo-capillary pressure curve was obtained from fine grid simulation of a single matrix block surrounded by fractures. For water-oil systems they present pseudo-capillary pressure curves for the matrix and fracture as:

$$P_{cowf} = \frac{S_{wf} k_z (\rho_o - \rho_w)}{L_z \sigma} \quad (2.16)$$

$$P_{cowm} = P_{cowf} + \frac{\phi}{\sigma} \frac{dS_{wm}}{dt} \left[ \frac{\mu_o}{k_{ro}} \right]_m$$

Here  $\sigma$  is same as that given by Kazemi et al. (1976). The value  $dS_{wm}/dt$  is found as a function of  $S_{wm}$  from fine grid simulation. This defines the matrix block recovery in the dual porosity simulation as the recovery from a single matrix block with uniform boundary conditions. This approach does not easily allow for variation of matrix block sizes or matrix rock properties throughout the reservoir. The reason behind this is that a fine grid solution of the saturation derivative would be required for any such variation in size or properties of the matrix.

Lim and Aziz (1995) derived matrix-fracture shape factors for single-phase flow by applying analytical solutions of the single-phase pressure diffusion equation for various parallelepiped geometries of the matrix blocks. Since the pressure diffusion equation governs the complete physics of fluid flow within the matrix block, therefore the shape factors obtained in this manner are physically and mathematically rigorous. A simple differential material balance within the matrix block can be used to show that the transfer function for single-phase flow is given as:

$$q_{mf} = -V \bar{\rho} \phi c_t \frac{\partial \bar{p}_m}{\partial t} \quad (2.17)$$

The time derivative in the above equation is obtained by solving the pressure diffusion equation within the matrix domain with appropriate boundary conditions (Lim and Aziz, 1995).

$$\frac{\partial p_m}{\partial t} = \frac{k}{\phi \mu c_t} \nabla^2 p_m \quad (2.18)$$

For example, for a matrix block surrounded by a set of parallel fractures separated by length  $L$  (fracture spacing), if the matrix is initially at a constant pressure and the pressure at the matrix-fracture boundary is suddenly reduced and maintained at a constant lower pressure, the solution of the above equation gives (Lim and Aziz, 1995):

$$\frac{\bar{p}_m - p_i}{p_f - p_i} = 1 - \frac{8}{\pi^2} \sum_{n=0}^{\infty} \frac{1}{(2n+1)^2} \exp\left[ \frac{-(2n+1)^2 \pi^2 kt}{\phi \mu c_i L^2} \right] \quad (2.19)$$

Since the complete diffusion equation is used, the assumption of pseudo-steady state is not made here. However, the above form of the solution has to be simplified in order that the final transfer function is simple and has a form similar to that given by Barenblatt (1960) and Warren and Root (1963), which is also the form of the transfer function used in current simulators. In order to do so, an exponential approximation of the above infinite series is used:

$$\frac{\bar{p}_m - p_i}{p_f - p_i} = 1 - 0.81 \exp\left[ \frac{-\pi^2 kt}{\phi \mu c_i L^2} \right] \quad (2.20)$$

Using this, the final transfer function is obtained as:

$$q_{mf} = \frac{\pi^2}{L^2} \frac{\bar{\rho} k_m}{\mu} (\bar{p}_m - p_f) \quad (2.21)$$

Thus, the new shape factor for a single set of fractures is derived as:

$$\sigma = \frac{\pi^2}{L^2} \quad (2.22)$$

It should be noted here that although the assumption of pseudo-steady state is not made in the derivation, the use of the exponential approximation results in the same consequence because the exponential approximation is not accurate in early time. In general for a parallelepiped matrix block, they derived the shape factor as:

$$\sigma = \frac{\pi^2}{(k_x k_y k_z)^{1/3}} \left[ \frac{k_x}{L_x^2} + \frac{k_y}{L_y^2} + \frac{k_z}{L_z^2} \right] \quad (2.23)$$

As mentioned before, although the above process is mathematically rigorous, it is so only for single-phase flow, and therefore the transfer function and shape factors so derived are only applicable to single-phase flow. Further, the shape factors are only derived for parallelepiped geometries and their use for other geometries is questionable.

Chang et al. (1993) have also avoided the pseudo-state assumption by combining the geometrical aspects of the systems with analytical solutions of the pressure diffusion equation for flow between the matrix and the fracture. However, the use of the transient diffusion equation leads to time-dependent shape factors. Using the complete solution to the diffusion equation, Chang et al. (1993) found the following equation for shape factor for one-dimensional flow:

$$\sigma = \frac{\pi^2 \sum_{m=0}^{\infty} \exp[-(2m+1)^2 \pi t_D]}{L_x^2 \sum_{m=0}^{\infty} \frac{1}{(2m+1)^2} \exp[-(2m+1)^2 \pi t_D]} \quad (2.24)$$

Here,

$$t_D = \frac{k_x t}{L_x^2 \phi \mu c_t} \quad (2.25)$$

The above shape factor converges asymptotically to the pseudo-steady state shape factor for dimensionless time greater than 0.1 as seen in Figure 2-3. Since real time equivalent to this is usually very small (for overall compressibility < 1e-5/psi and typical reservoir parameters), it might sometimes be plausible to only use the pseudo-steady state shape factor.

However, for reservoirs with overall compressibility much higher, for example gas and gas condensate reservoirs with compressibility around 1e-2/psi, real time equivalent of 0.1

dimensionless time could be around 10 days. Thus, the pseudo-steady state approximation would not be valid at early time. This can have significant effects in the analysis of transient well tests in such reservoirs, because such tests usually last for 1-2 days and would thus fall in this transient period. Further more, for tight gas reservoirs transients can last for many months, implying that even full field simulations would be prone to error if transients are not accounted for.

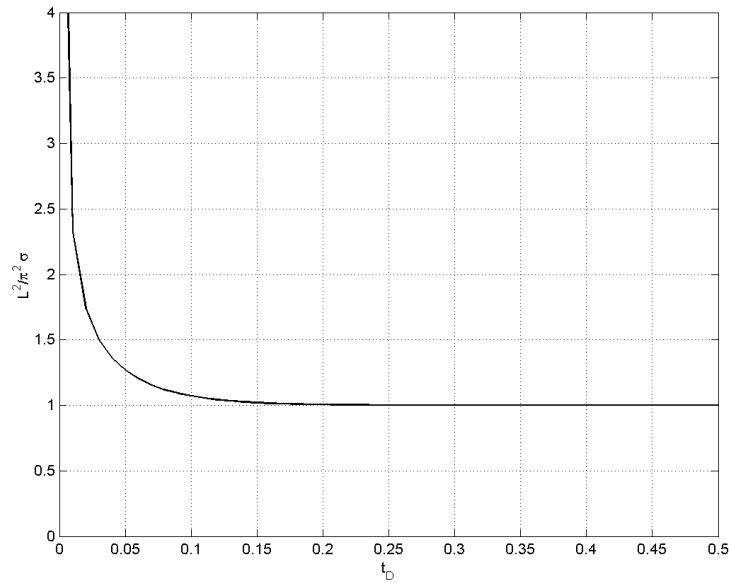


**Figure 2-3** Variation of transient shape factor with time

Although the Chang et al. (1993) model accounts for transient flow and gives an analytical form of the transient shape factor, the expression is too complicated to be incorporated directly into simulators. And again, there is the question of validity of such expressions for non-orthogonal systems.

Sets of Fractures	Warren and Root	Kazemi et al.	Coats et al.	Lim and Aziz
1	12	4	8	$\pi^2(9.87)$
2	32	8	16	$2\pi^2(19.74)$
3	60	12	24	$3\pi^2(29.61)$

**Table 2-1** Shape factor constant given by various researchers for 1, 2 and 3

sets of fractures (Lim and Aziz, 1995)

There are many other values of the shape factors available in literature, derived based upon different assumptions. It would be impossible to discuss all of them in detail. The above table gives some of the prominent values of the shape factor constant,  $a$ , where the shape factor is given by  $a/L^2$ .

All of these are derived with an inherent assumption of pseudo-steady state (Lim and Aziz, 1995). It's also obvious that they are only defined for orthogonal systems.

## 2.4. The Current Transfer Function

The last section discussed the dual porosity formulations proposed by various authors for multiphase immiscible flow. We observed that the only difference in the various models was the way the total potential (pressure, capillary pressure and gravity) in the transfer function was calculated. This formulation can be directly extended to compositional dual porosity/dual permeability systems, which is the most general form. By using a material balance on the components, it can be shown that the finite difference form of the matrix-fracture equations for a control volume with 'ns' surfaces is given as (Aziz, 2001):

$$\left\{ \left\{ \sum_{s=1}^{ns} [T_s \sum_p (\lambda_p \rho_p X_{cp} \Delta \Phi_p)_s] + WI^W \cdot \sum_p [\lambda_p \rho_p X_{cp} (p_p - p^W)] \right\}^{n,n+1} \right\}_m - \tau_{c_{mf}} \quad (2.26)$$

$$= \left\{ \frac{\phi^{n+1} \sum_p (S_p \rho_p X_{cp})^{n+1} - \phi^n \sum_p (S_p \rho_p X_{cp})^n}{\Delta t} \right\}_m$$

$$\left\{ \left\{ \sum_{s=1}^{ns} [T_s \sum_p (\lambda_p \rho_p X_{cp} \Delta \Phi_p)_s] + WI^W \cdot \sum_p [\lambda_p \rho_p X_{cp} (p_p - p^W)] \right\}^{n,n+1} \right\}_f + \tau_{c_{mf}} \quad (2.27)$$

$$= \left\{ \frac{\phi^{n+1} \sum_p (S_p \rho_p X_{cp})^{n+1} - \phi^n \sum_p (S_p \rho_p X_{cp})^n}{\Delta t} \right\}_f$$

In the above equations,  $\Delta\Phi_p$  denotes phase potential difference (Aziz, 2001). The RHS is the accumulation part, the first term on the LHS is the flux through all the surfaces of the control volume, the second term on the LHS is the well flux, and  $\tau_{c_{mf}}$  is the transfer function. Notice that the matrix equation also has flux terms that are a result of the dual permeability assumption, meaning that the matrix blocks are also connected to each other. Subscript  $c$  in the above equations stands for component. There are as many equations per gridblock as the number of components.

If the matrix and matrix block face pressures can be approximated by their values at grid nodes then the transfer function is given as (Aziz, 2001):

$$\tau_{c_{mf}} = k_m \sigma V \sum_p \left[ \lambda_p \rho_p X_{cp} (\Phi_{pm} - \Phi_{pf}) \right] \quad (2.28)$$

Here,  $\Phi_p$  is the total potential incorporating pressure diffusion, imbibition and gravity segregation and is usually equal to the potential given by Kazemi et al. (Equation 2.7) or Litvak (Equation 2.13).

## 2.5. Multiple Sub-domain Formulations

This section discusses the class of dual porosity formulations that discretize the matrix block in order to have a better resolution of the pressure and saturation distribution and incorporate transient effects. These formulations apply the single porosity flow equations over the discretized matrix domain, allowing pressure and saturation distributions to be calculated to a finer resolution within the matrix block, while the mass transfer between the fractures and connected matrix subdomains is given by the dual porosity transfer function.

Gilman (1986) presented a method of matrix block grid refinement that allows saturation fronts to exist within the matrix blocks. His method refines the matrix block into subdomains with the transfer between matrix subdomains and the neighboring fracture described in the conventional manner via dual porosity transfer functions for each matrix subdomain. The finite difference form of his formulation is given as:

$$\left\{ \sum_l T_l \lambda_p \rho_p \Delta (p_p - \gamma_p D) + \rho_p q_p^w \right\}_f - \sum_{N_m} \tau_{mf} = \left\{ \frac{V}{\Delta t} \Delta_t (\phi S_p \rho_p) \right\}_f \quad (2.29)$$

$$\left\{ \sum_l T_l \lambda_p \rho_p \Delta (p_p - \gamma_p D) + \rho_p q_p^w \right\}_m + \tau_{mf} = \left\{ \frac{V}{\Delta t} \Delta_t (\phi S_p \rho_p) \right\}_m \quad (2.30)$$

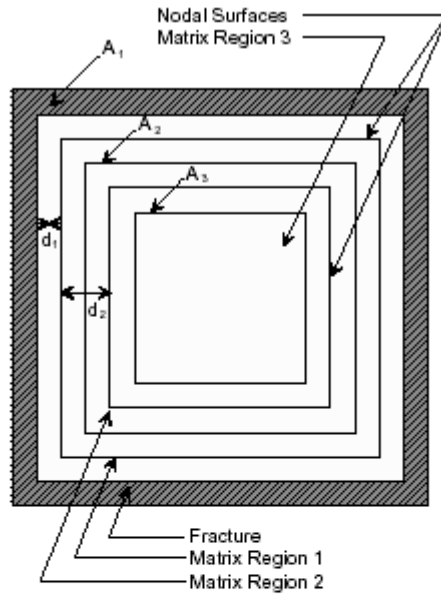
The summation in Equation 2.29 is because of mass transfer from multiple subdomains into the fracture, which is possible for stacked matrix blocks (Figure 2-4b).  $\tau_{mf}$  can be set to zero for any matrix subdomain that is not connected to the fracture, which would be the case for all internal subdomains for a nested system (Figure 2-4a). The transfer function is given as:

$$\tau_{mf} = k_m V \sigma \left\{ \omega_p \lambda_{pm} + (1 - \omega_p) \lambda_{pf} \right\} \rho_p \left[ (p_p - \gamma_p D)_f - (p_p - \gamma_p D)_m \right] \quad (2.31)$$

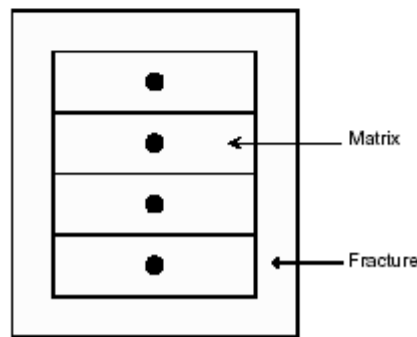
The transmissibilities between fractures and between matrix subdomains are same as for single porosity systems. Besides allowing one to relax the assumption of pseudo-steady matrix/fracture flow, matrix subdomains give a more accurate modeling of phase segregation effects that can occur in naturally fractured reservoirs. Gilman (1986) does not present any field scale simulations using this method. The largest case he presented is a one dimensional, horizontal waterflood with ten fracture nodes and five matrix subdomains per fracture node. This represents a total of 50 computational nodes. He does present some possible computational times for field scale simulations and shows that for simulations where the matrix solution time is 75 percent of the total simulation run time, the five subdomain formulation will increase computing time by 50 percent. Since the jacobian is split to solve the fracture and matrix unknowns sequentially instead of simultaneously solving for both the matrix and fracture unknowns at once, using matrix subdomains may not cause unreasonable simulation times while maintaining a fully implicit nature. However, this can lead to stability problems.

Another matrix-subdomain formulation for dual porosity reservoirs is the Multiple Interacting Continua method (MINC) proposed by Pruess and Narasimhan (1985). This method lumps matrix volumes into subdomains based upon the distance to the nearest fracture. They implemented this formulation using an Integral Finite Difference (IFD) method. The advantage IFD has over the standard finite difference scheme is in its flexible handling of domain geometries. IFD is readily adapted to non-parallelepiped matrix blocks unlike the various double porosity schemes previously discussed. For a single component system the mass transport equation is given as:

$$\frac{d}{dt} \int_V \rho \phi dV = \int_S \vec{F} \cdot \vec{j} dS + \int_V q dV \quad (2.32)$$



(a): MINC-partitioning



(b): Subdomain partitioning

**Figure 2-4** Dual porosity grid system with matrix subdomain decomposition (CMG, 2002)

This is defined for any arbitrary region  $V$  with surface area  $S$ . The mass flux  $F$  is given by Darcy's law as usual. The volume integrals are replaced by appropriate volume averages and the surface integral is approximated with a discrete sum of volume elements as:

$$\begin{aligned}
 \int_V \rho \phi dV &= \phi_j V_j \\
 \int_S \vec{F} \cdot \vec{j} dS &= \sum_m F_{jm} A_{jm}
 \end{aligned}
 \tag{2.33}$$

Approximating the time derivatives by first order finite differences:

$$\left(\phi_j^{n+1} \rho_j^{n+1} - \phi_j^n \rho_j^n\right) - \frac{\Delta t}{V_j} \left[ \sum_m F_{jm}^{n+1} A_{jm} + V_j q_j^{n+1} \right] = 0 \quad (2.34)$$

To complete the formulation, expressions for V and A are required for a particular domain.

Wu and Pruess (1986) presented comparisons of the MINC formulation to conventional dual porosity formulations. They found that at early times the dual porosity formulation tends to underestimate the imbibition transfer rate because the capillary pressure difference in the dual porosity formulation is applied over a larger length than with the MINC formulation. This results in a lower capillary gradient in the dual porosity formulation and a lower matrix/fracture imbibition rate. At intermediate times the MINC imbibition rate is lower than that predicted from a dual porosity formulation due to the build up of water at the matrix/fracture interface. This water build up reduces the capillary pressure at the matrix/fracture interface thereby reducing the matrix/fracture imbibition rate. Figure 2-5 shows the imbibition recovery and imbibition rate from a 10x10x30 foot matrix block immersed in water. Comparisons of the results from a MINC simulation and a double porosity formulation are shown in this is figure (Wu and Pruess, 1986). However, it is interesting to note that for a field scale simulation carried out comparing the MINC and the dual porosity formulations, very little difference is found in the results (Wu and Pruess, 1986).

The major limitation of multiple subdomain formulations for naturally fractured reservoirs is the potentially huge number of computational nodes required if significant numbers of matrix blocks require gridding into subdomains. Although, it is not proposed that all the matrix blocks within the reservoir be gridded, even gridding a " representative " matrix block within a gridblock is potentially computationally tenuous.

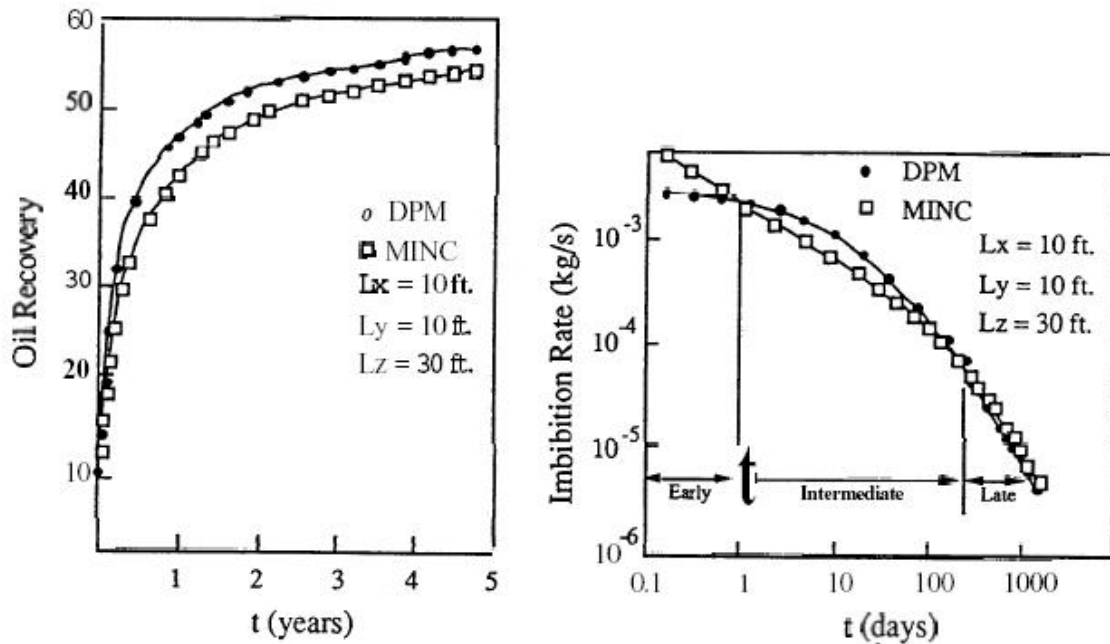


**Figure 2-5** Oil recovery and imbibition rate for rectangular matrix block (Wu and Pruess, 1986)

Further, determination of what a “representative” matrix block should be when there are possibly thousands of matrix blocks within the gridblock is not well defined. Using a single “representative” matrix block within a gridblock will not allow the many different imbibition or drainage rates one would expect with multiple matrix blocks within the gridblock. These differences in transfer rate from one matrix block to another within a computational gridblock would be caused by different exposure times to fracture water in the case of imbibition or lower saturations in the up-structure matrix blocks as compared to the down-structure matrix blocks during gravity drainage. Gridding of multiple matrix blocks within the gridblock would resolve these problems somewhat but at a possibly prohibitive computing cost (Beckner, 1990).

## 2.6. Summary

This chapter presented a historical perspective of the development of the dual porosity formulation for simulating naturally fractured reservoirs, along with a discussion of the advantages and limitations of many different formulations and extensions. It is shown that the dual porosity formulations existing today suffer fundamentally from their inability to model multiphase flow accurately, due to the fact that the existing models are

not physically and mathematically rigorous for multiphase flow, but are direct extensions of the single phase flow equations. Such an extension is not physically valid because of additional mechanisms that govern multiphase flow. Further, it is seen that the shape factors derived so far are only meant for parallelepiped matrix blocks and pseudo-steady state flow. Although researchers have acknowledged the time dependence of the shape factor for transient flow, a useful and simple expression for transient shape factors has not yet been developed. Also, their use for other non-orthogonal geometries has not been studied and is questionable. However, it is common knowledge that for many typical NFRs, fractures are far from orthogonal.

Attempts to increase resolution and accuracy of dual porosity models by use of matrix subdomains, is, although a useful concept, results in potentially prohibitive computational costs. Thus, the development of a dual porosity formulation more representative of multiphase flow and the capability to derive shape factors for any arbitrary matrix shape that takes into account both transient and pseudo-steady state flow is required, and is the major focus of this study.

## **Chapter 3**

### **3 Single Phase Mass Transfer**

We have through the last chapter motivated the need for improved shape factors that take into account both transient and pseudo-steady state flow for any arbitrary matrix-fracture

geometry. This chapter starts with a discussion of the mechanisms of single-phase mass transfer and then defines a differential form of the transfer function. The limitations of current shape factors for single-phase flow are then discussed in detail and to further motivate the want for new shape factors, effects of transient flow and non-orthogonal systems are shown through simple test cases. Combining the differential form of the single-phase transfer function and the single-phase pressure diffusion equation, an analytical form for a shape factor for transient pressure diffusion is derived. Further, a pseudo-steady state shape factor for rhombic fracture systems is also derived. Finally, a general numerical technique to calculate the shape factor for single-phase flow for any arbitrary shape of the matrix (i.e. non-orthogonal fractures) is proposed. This technique also accounts for both transient and pseudo-steady state pressure behavior. The results were verified against fine-grid single porosity models and were found to be in excellent agreement.

### **3.1. Mechanisms of Mass Transfer**

It has been mentioned earlier that the gamut of mechanisms of mass transfer for a dual porosity media with multiphase flow include fluid expansion or pressure diffusion, imbibition or saturation diffusion, gravity imbibition or drainage, mass diffusion and viscous displacement or convection (ECLIPSE 100 Technical Description, 2000). However, for single-phase flow, it is obvious that imbibition, gravity forces and mass diffusion do not exist, and thus leaving only fluid expansion and viscous displacement as the mechanisms of mass transfer.

To further understand the dominating mechanisms, let us conceptualize a simple theoretical fractured reservoir with single-phase flow, as depicted by Figure 3-1. The figure shows rectangular matrix blocks with thin fractures on all sides, a source (injector) in red and a sink (producer) in green.

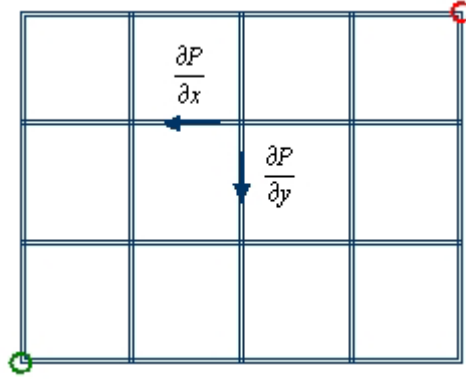


**Figure 3-1** Conceptual representation of a fractured reservoir with sources and sinks

Due to the presence of sources and sinks, there would be pressure gradients in the system, and for single porosity systems, these pressure gradients are the major forces driving flow. However, for dual porosity systems, because the fractures are much more permeable as compared to the matrices, these pressure gradients would more or less be parallel to the fractures. Thus, their effect on mass transfer between fracture and matrix would be negligible, implying that viscous displacement can be neglected for dual porosity mass transfer. With this assumption, the only force that is left for single-phase flow is fluid expansion. Hence, any transfer function defined for single-phase flow would be accurate if it can take fluid expansion into account rigorously.

### 3.2. Single Phase Transfer Function

Consider an arbitrary shaped matrix block of volume  $V$  and porosity  $\phi$  surrounded by fractures on all sides and filled with a compressible fluid. If at any give time, the density of the fluid is  $\bar{\rho}$ , and after a time  $dt$ , the density is  $\bar{\rho} - d\bar{\rho}$ , then the mass transfer between the fractures and the matrix over time  $dt$  is given as:

$$\begin{aligned}
 &= V\phi(\bar{\rho} - d\bar{\rho}) - V\phi\bar{\rho} \\
 &= -V\phi d\bar{\rho}
 \end{aligned} \tag{3.1}$$

Thus, the rate of matrix-fracture mass transfer is given as:

$$q_{mf} = -V\phi \frac{\partial \bar{\rho}}{\partial t} \quad (3.2)$$

Compressibility is defined in terms of pressure as (Aziz, 2001):

$$\frac{\partial \rho}{\partial t} = \rho c \frac{\partial p}{\partial t} \quad (3.3)$$

Using this definition, we finally have:

$$q_{mf} = -V\phi \bar{\rho} c \frac{\partial \bar{p}}{\partial t} \quad (3.4)$$

This is the differential form of the transfer function valid for single-phase flow pertinent to the above assumptions. However, it is not feasible to incorporate this form of the transfer function directly into a simulator. The pressure derivative has to be calculated to finally arrive at a transfer function similar in form to that given by Barenblatt et al. (1960), which is very simple and its incorporation into existing simulators is relatively easy.

### 3.3. Limitations of Existing Models

As we saw in the previous chapter, although the form of the transfer function is correct for single-phase flow, there are two major limitations of the shape factors:

- Most of the derivations of the existing shape factors either assume that the matrix-fracture system is always at pseudo-steady state, or take exponential approximations of the full solution (Lim and Aziz, 1995) which has the same consequence. As mentioned before, there is a finite amount of time initially when the system is in a transient state, and this period can be significant for highly compressible reservoirs like gas reservoirs or low permeability tight reservoirs, and for such systems the transients have to be taken into account.

- All existing shape factors have only been derived for parallelepiped matrix blocks or orthogonal fracture systems. Their use for other non-orthogonal geometries has not been studied and is questionable. However, it is common knowledge that for many typical NFRs, fractures are far from orthogonal.

In order to have a clear understanding of these limitations, two test cases will be discussed. The first case shows the limitations of pseudo-steady state shape factors, and the second the differences in system responses as a result of non-orthogonality.

Consider a 10x10x10 cu-ft cubic matrix block with a single set of fractures as shown in Figure 3-2. This system is filled with a compressible single-phase fluid and is initially at a constant pressure of 1000 psi.

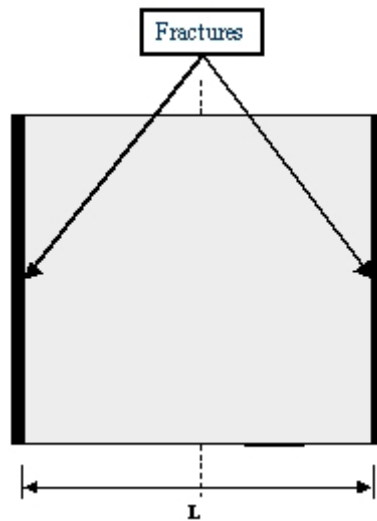


**Figure 3-2** Cubic matrix with a single set of fractures (figure from Rangel-German, 2002)

The system is subjected to a pressure drawdown by reducing fracture pressures suddenly to 500 psi and maintaining them at this constant pressure. Figure 3-3 shows the reduction of average pressure within the matrix block with time. The blue curve (with crosses) is obtained using a fine grid model with ECLIPSE 100 and is the reference solution. The other curves are obtained using ECLIPSE 100 dual porosity model, with various constant shape factors given in Table 2-1. It is observed that none of the dual porosity curves match the reference, especially during early time, although the match becomes better with

time and asymptotically reach the reference solution. Further, we see that as the magnitude of the shape factor increases (Table 2-1), the match becomes better and better, but even the largest shape factor given by Warren and Root (1963) initially gives a lower pressure drop and later on a larger pressure drop than the reference solution, meaning that the curves intersect each other. We also see that during early time the pressure drop for the reference solution is maximum, implying that all the shape factors are smaller than that required to produce the necessary mass transfer rate. From all this, it is clear that a constant value of the shape factor cannot be used to produce a good match at all times. The reason behind this discrepancy is the existence of a transient state during early time, during which all these shape factors based on the pseudo-steady state assumption are invalid.

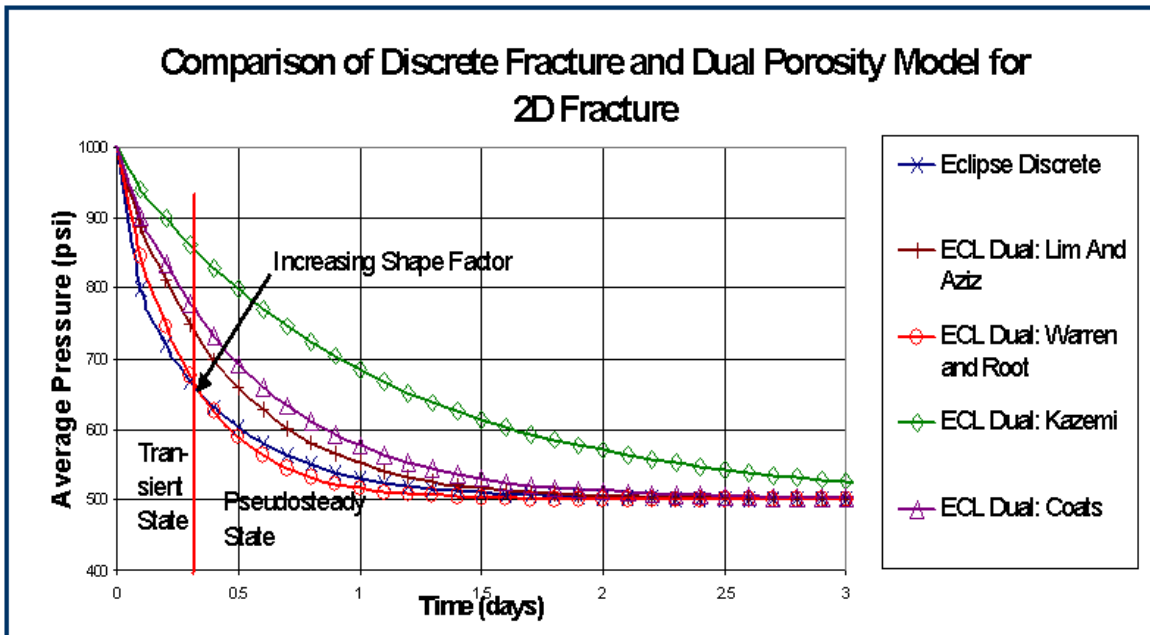


**Figure 3-3** Comparison of pressure drawdown of discrete fracture model and dual porosity models

For this particular example, the transient exists only for a few hours. But as mentioned before, for highly compressible reservoirs or tight reservoirs, this transient can last for many days or even months. It is thus essential that the transient state be modeled accurately for such reservoirs.

To understand the effect of non-orthogonal fracture systems, consider a pressure drawdown on a rhombic matrix block. If we have to model such a rhombic system with an orthogonal one, then the closest approximation would be a cubic matrix block of equal volume. These two models are shown in Figure 3-4 and 3-5. Both systems are subjected to the same initial and boundary conditions as in the previous example.

Figure 3-6 shows the average pressure response of the two systems. It is observed that the drawdown of the rhombic system is significantly more than that for the cubic system, implying greater rates of mass transfer (around 10% more for this system), although their volumes are the same. This can be attributed to the fact that the fracture surface area is greater for the rhombic system.

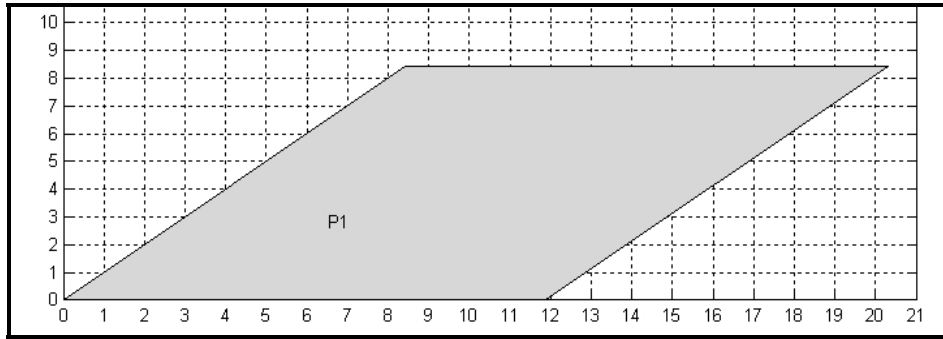


**Figure 3-4** A Rhombic matrix block

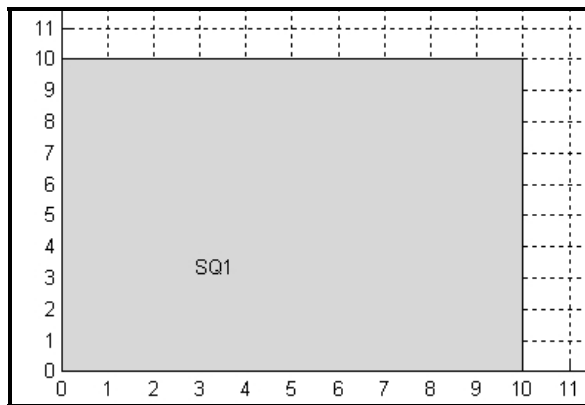


**Figure 3-5** An equivalent square matrix block

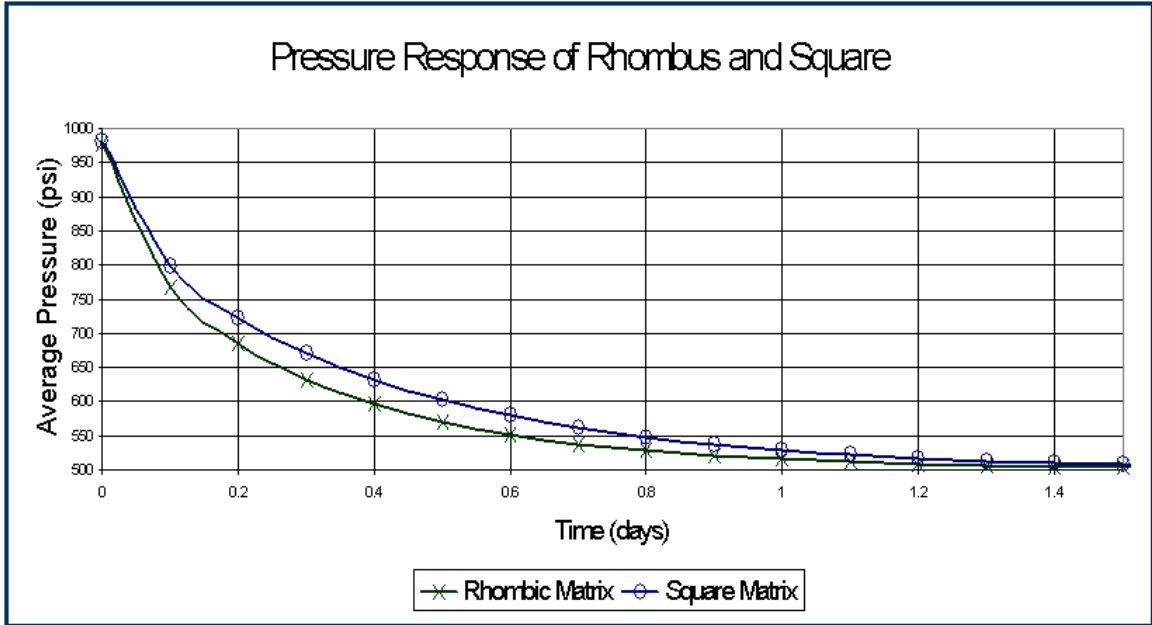


**Figure 3-6** Pressure response of rhombic and square matrix blocks

Thus, it would be reasonable to conclude that in some situations, transient and/or non-orthogonal effects may be important, and therefore it might be necessary to model them for an improved representation of the NFR.

### 3.4. Transient Pressure Behavior

Transient flow from a matrix-fracture standpoint is defined as the time until which any pressure disturbance caused by any change in boundary condition at any boundary (fracture) has not “felt” the effect or presence of other boundaries. In order to model transient flow behavior, a transient shape factor has to be derived. This derivation is based on the use of the complete single-phase pressure diffusion equation as used by Lim and Aziz (1995). But the boundary conditions used here are defined to model transient flow only. Since the effect of other boundaries is not felt in this regime, transient flow theoretically can thus be modeled simply as one-dimensional flow in a semi-infinite domain. Figure 3-7 depicts the matrix abstraction to model transient flow.

The matrix-fracture system is infinite in extent along the y-axis, and the matrix extends to infinity along the positive x-axis. The diffusion equation that governs flow within this matrix block is given as:

$$\frac{\partial p}{\partial t} = D \frac{\partial^2 p}{\partial x^2} \quad (3.5)$$

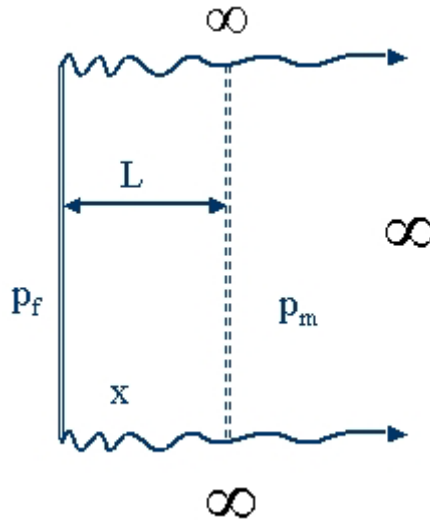


**Figure 3-7** Matrix abstraction to model transient flow

Here  $D$  is the hydraulic diffusivity given as:

$$D = \frac{k}{\phi \mu c_t} \quad (3.6)$$

The boundary and initial conditions are given as:

$$p(0, t) = p_f \quad p(\infty, t) = p_m \quad p(x, 0) = p_m \quad (3.7)$$

Using the following non-dimensionalizations (Shaqfeh, 2001):

$$P = \frac{p - p_f}{p_m - p_f} \quad \eta = \frac{x}{2\sqrt{Dt}} \quad (3.8)$$

Equation 3.5 reduces to the following ODE (Shaqfeh, 2001):

$$-2\eta P = P'' \quad P(0) = 0, P(\infty) = 1 \quad (3.9)$$

The solution of the above system is quite well known and is given as (Shaqfeh, 2001):

$$P(\eta) = \text{erf}(\eta) \quad (3.10)$$

Since we now have the entire pressure solution within the matrix block, we can easily calculate the volumetric average pressure within the matrix block of length  $L$  and its time derivative:

$$\bar{P}(\eta_L) = 1 + \frac{1}{\eta_L} \left[ a \text{Ei}(\eta_L^2) - b \right] \quad (3.11)$$

$$\frac{\partial \bar{P}}{\partial \eta_L} \propto \frac{1 - \bar{P}}{\eta_L} \quad (3.12)$$

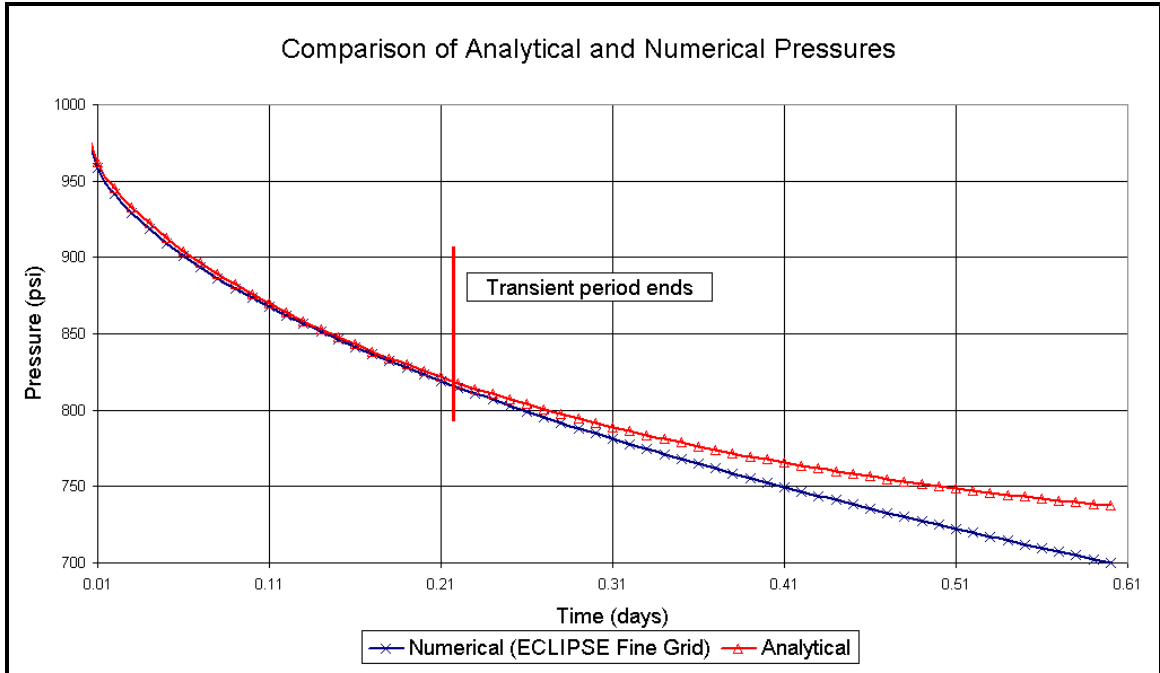
Here  $\text{Ei}$  is the exponential integral, and  $a$  and  $b$  are constants. Combining Equation 3.12 with the definition of the transfer function given by Equation 3.4, we have the final definition of the shape factor as:

$$\sigma = \frac{1}{2Dt} \left[ \frac{1}{\bar{P}} - 1 \right] \quad (3.13)$$

The important observation here is that the shape factor is now no longer a constant but a function of time, i.e., it is inversely proportional to time when the system is in a transient state.

$$\sigma \propto \frac{1}{t} \quad (3.14)$$

This nature of time dependence agrees with the simulation results of the previous section, and also with the results of Chang et al. (1993) as seen in the previous chapter.



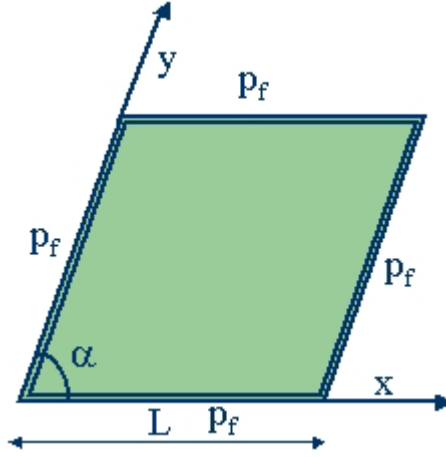
**Figure 3-8** Comparison of numerical and analytical pressure response for a cubic matrix block

Figure 3-8 shows a comparison of the average matrix pressures for a cubic matrix block subjected to a pressure drawdown, the blue curve (with crosses) obtained numerically using ECLIPSE 100 fine grid model (reference solution), and the red curve (with triangles) obtained using the analytical solution proposed above. We see that indeed during the transient state of the system, the analytical solution matches the reference solution very well, but when pseudo-steady state is reached, the analytical transient solution is no longer valid, and the pseudo-steady state shape factor has to be used after this time.

This section gave a mathematical basis to our understanding of transient matrix-fracture flow and verified the time dependence of the shape factor. We will later propose a numerical algorithm capable of calculating this transient shape factor for any shape of the matrix block.

### 3.5. Non-orthogonal Fracture Networks

We have earlier seen the effects of non-orthogonality through the simple example of a rhombic matrix system. This section presents a mathematical derivation of the shape factor for such a non-orthogonal rhombic system. The rhombic matrix abstraction is shown in the figure below:



**Figure 3-9** The rhombic matrix abstraction

The methodology is again to solve the single-phase pressure diffusion equation within the matrix block. A covariant coordinate transformation of the normal 2D coordinate system is used in order that the boundary and initial conditions are transferred to surfaces of constant coordinate in the new coordinate system. This makes the solution procedure relatively easy. If  $(\hat{x}, \hat{y})$  represents the normal coordinate system and  $(x, y)$  represents the new coordinate system, then:

$$\hat{y} = y \sin \alpha \quad \hat{x} = x + y \cos \alpha \quad (3.15)$$

With this definition, the dimensionless form of the pressure diffusion equation in 2D can be written as:

$$\frac{\partial P}{\partial \tau} = \frac{\partial^2 P}{\partial X^2} + \frac{1}{\sin^2 \alpha} \frac{\partial^2 P}{\partial Y^2} \quad (3.16)$$

The dimensionless variables are:

$$P = \frac{p - p_f}{p_m - p_f} \quad \tau = \frac{Dt}{L^2} \quad X = \frac{x}{L} \quad Y = \frac{y}{L} \quad (3.17)$$

The boundary and initial conditions are the same as those used by Lim and Aziz (1995):

$$\begin{aligned} P(0, Y, \tau) = 0, P(1, Y, \tau) = 0, P(X, 0, \tau) = 0, \\ P(X, 1, \tau) = 0, P(X, Y, 0) = 1 \end{aligned} \quad (3.18)$$

The above system is solved using separation of variables (Crank, 1975, Carslaw et al., 1959). Since the entire pressure solution within the matrix block is now available, the volumetric average pressure can be easily calculated, and it is given as:

$$\bar{P}(\tau) = \frac{4}{\pi^4 \sin \alpha} \sum_{n=1}^{\infty} \sum_{m=1}^{\infty} \frac{1}{n^2 m^2} (1 - \cos n\pi)^2 (1 - \cos m\pi)^2 \exp(-\lambda_{nm}^2 \tau) \quad (3.19)$$

$$\lambda_{nm}^2 = \frac{\pi^2}{\sin^2 \alpha} (m^2 + n^2 \sin^2 \alpha) \quad (3.20)$$

Again, since the above solution is an infinite series, we need to use its asymptotic approximation, but that again results in consequences similar to using the pseudo-steady state assumption (Lim and Aziz, 1995).

$$\bar{P}(\tau) = \frac{64}{\pi^4 \sin \alpha} \exp \left[ \left\{ \frac{-\pi^2}{\sin^2 \alpha} (1 + \sin^2 \alpha) \right\} \tau \right] \quad (3.21)$$

Equation 3.21 can be used to calculate the time derivative of the average pressure, and this in conjunction with the differential form of the transfer function (Equation 3.4) gives the transfer function as:

$$q_{mf} = \frac{\pi^2}{L^2 \sin^2 \alpha} \left[ 1 + \sin^2 \alpha \right] \frac{V \bar{\rho} k}{\mu} (\bar{p} - p_f) \quad (3.22)$$

Thus the 2D (2 sets of fractures in the x-y plane) pseudo-steady state shape factor for a rhombic system is given as:

$$\sigma = \frac{\pi^2}{L^2 \sin^2 \alpha} [1 + \sin^2 \alpha] \quad (3.23)$$

We observe that for  $\alpha = 90^\circ$ , this shape factor becomes the same as that derived by Lim and Aziz (1995) and Chang et al. (1993).

The same methodology can be easily applied to a 3D rhombic system with vertical fractures, i.e., for a rhomboid with side length  $L$  (vertical sides in the  $Z$  direction), the shape factor is given as:

$$\sigma = \frac{\pi^2}{L^2 \sin^2 \alpha} [2 + \sin^2 \alpha] \quad (3.24)$$

Now, in order to understand the effect of non-orthogonality, consider the ratio of the 2D shape factors for such a rhombic system and a cubic system of equal fracture lengths:

$$\frac{\sigma_R}{\sigma_C} = \frac{1 + \sin^2 \alpha}{2 \sin^2 \alpha} \quad (3.25)$$

If, say the angle  $\alpha = 30^\circ$ , the above ratio is equal to 2.5, and becomes larger and larger as  $\alpha$  tends to zero. Thus we realize that if everything else is the same, just by changing the angle between the fractures, the rate of mass transfer can be varied tremendously. We can thus conclude that non-orthogonality of fractured systems has to be taken into account for accurate modeling of NFRs. It should be noticed here that we are not comparing a cubic and a rhombic system of equal volume but of equal fracture lengths, unlike Section 3.3. This is done in order understand specifically the effect of non-orthogonality alone. However, if we have to approximate a rhombic system with a cubic one, then the best approximation as mentioned before is by a cubic system of equal volume as the rhombic system. In this case the ratio becomes:

$$\frac{\sigma_R}{\sigma_C} = \frac{1 + \sin^2 \alpha}{2 \sin \alpha} \quad (3.26)$$

For  $\alpha = 30^\circ$ , the ratio now is 1.25, that is, the rate of mass transfer for the rhombic system is 25% more than the cubic system. Although this is not as large as before, it is still a significant amount. And again, this ratio becomes larger as  $\alpha$  becomes smaller.

### 3.6. A Generic Shape Factor Formulation

We have throughout the last sections motivated the need for shape factors that can take into account transient flow and non-orthogonal fracture systems. This section presents a simple numerical algorithm that can be used to calculate the shape factor for any arbitrary matrix block and account for both transient and pseudo-steady state flow. However, the present version of the software can directly calculate the shape factors only for 2D matrix-fracture systems. An indirect system to calculate the shape factor for 3D systems will be discussed.

The algorithm is based on the simple observation that the final form of the transfer function for single-phase flow is always given as:

$$q_{mf} = \sigma V \bar{\rho} \frac{k_m}{\mu} (\bar{p}_m - p_f) \quad (3.27)$$

The differential form of the transfer function is given as:

$$q_{mf} = -V \bar{\rho} \phi c_t \frac{\partial \bar{p}_m}{\partial t} \quad (3.28)$$

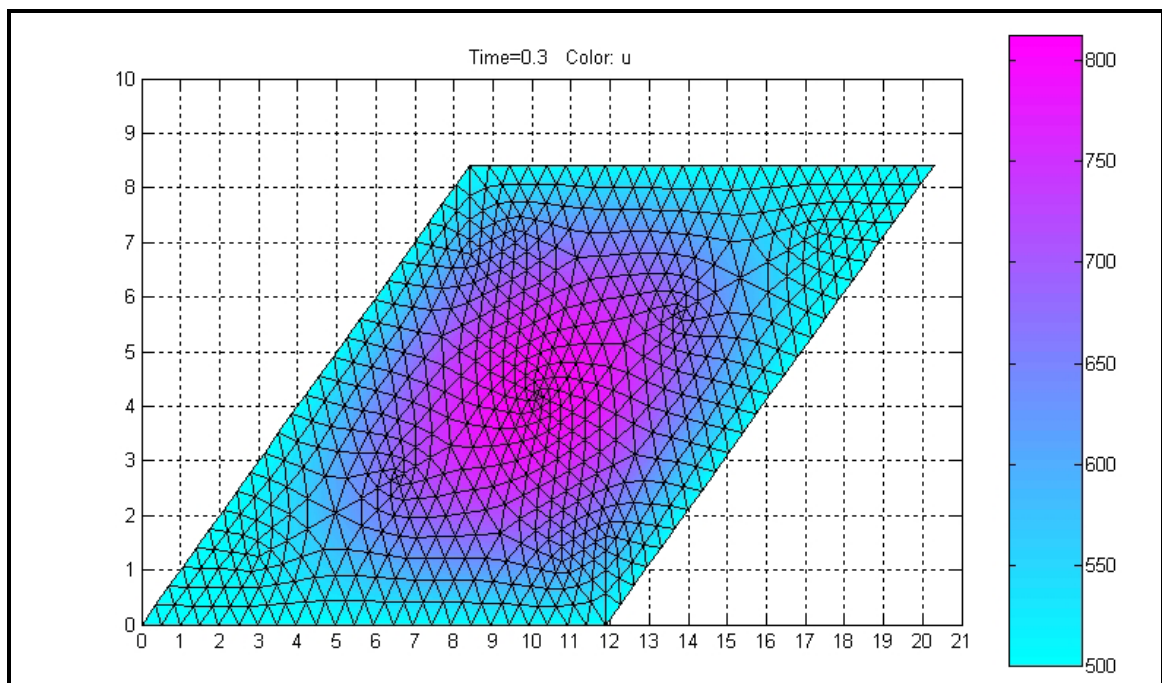
Combining the above two equations we have the following definition of the shape factor:

$$\sigma = -\frac{1}{D(\bar{p}_m - p_f)} \frac{\partial \bar{p}_m}{\partial t} \quad (3.29)$$

Thus, all that is required is to calculate the pressure solution within a given matrix block numerically, and then the average pressure and its time derivative can also be calculated to finally arrive at the shape factor as a function of time. The algorithm is as follows:

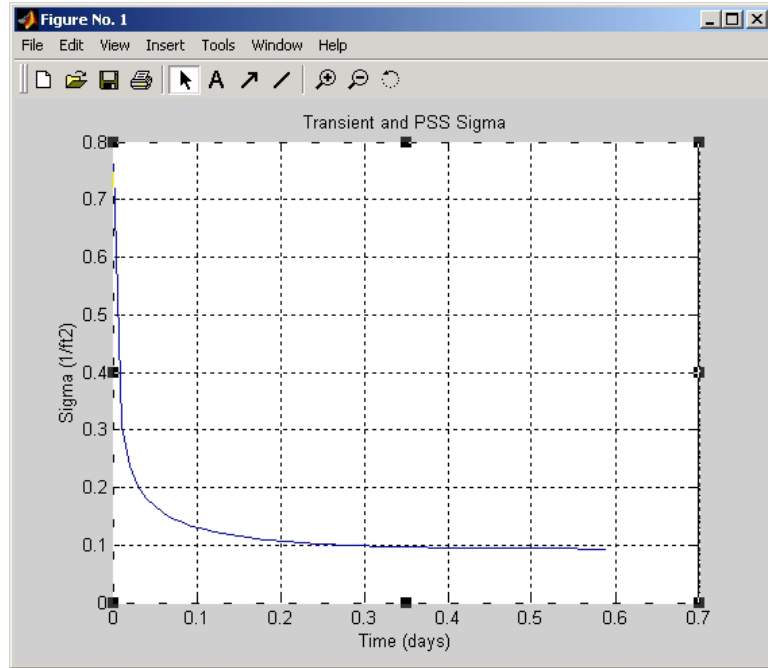
1. Take any given matrix block (shape and size) as input and discretize it into grids. The software developed uses Matlab PDE Toolbox to grid the given matrix. Triangular grids are used.
2. Solve for pressure within the given matrix block using any PDE solver with Dirichlet boundary conditions and uniform initial conditions. The software developed uses the Matlab PDE Toolbox.
3. Calculate the volume average pressure for the matrix block.
4. Calculate the derivative of the average pressure numerically. If necessary, smooth the data so obtained.
5. Calculate  $\sigma$  from Equation 3.29.

Figure 3-10 shows the pressure solution obtained within a rhombic matrix block using the Shape Factor Software (Appendix A) developed with Matlab Release 12 (MathWorks, 1996).



**Figure 3-10** Pressure solution using Matlab PDE Toolbox

Figure 3-11 shows the calculation of the shape factor using the above algorithm.  $\sigma$  is initially varying with time in the transient state and finally becomes constant and equal to the shape factor derived by Lim and Aziz (1995) and Chang et al. (1993) when pseudo-steady state is reached.



**Figure 3-11** The shape factor for a rhombic matrix block calculated numerically

As mentioned before, one limitation of the software developed is that it can only be used for 2D matrix-fracture systems directly, as the Matlab PDE Toolbox (MathWorks, 1996) can only be used to solve 2D systems. However, an indirect technique can be used to calculate 3D shape factors. This technique is based on the observation that because linear superposition of the pressure solution is applicable (both the governing PDE and boundary conditions are linear), the total 3D shape factor is given as:

$$\sigma_{xyz} = \sigma_x + \sigma_y + \sigma_z \quad (3.30)$$

Thus, the shape factor for flow in the x-y plane can be solved as above, and the shape factor for flow in the z direction can also be obtained by the same technique. Both of these can be added to calculate the 3D shape factor.

To verify the above concept, consider a 10x10x10 ft matrix block with a 2D fracture system in the x-y plane. The 2D shape factor would thus be given by:

$$\sigma_{xy} = \sigma_x + \sigma_y \quad (3.31)$$

Since the side lengths are same in the x and y directions for this case, therefore  $\sigma_x = \sigma_y$ .

Thus, we have:

$$\sigma_{xy} = 2\sigma_x \quad (3.32)$$

The numerical algorithm is used to calculate the shape factor directly in 2D (reference solution) and then in 1D (x direction), by converting the y direction boundary conditions from Dirichlet to Neuman boundary conditions. The results are shown in Figure 3-12.

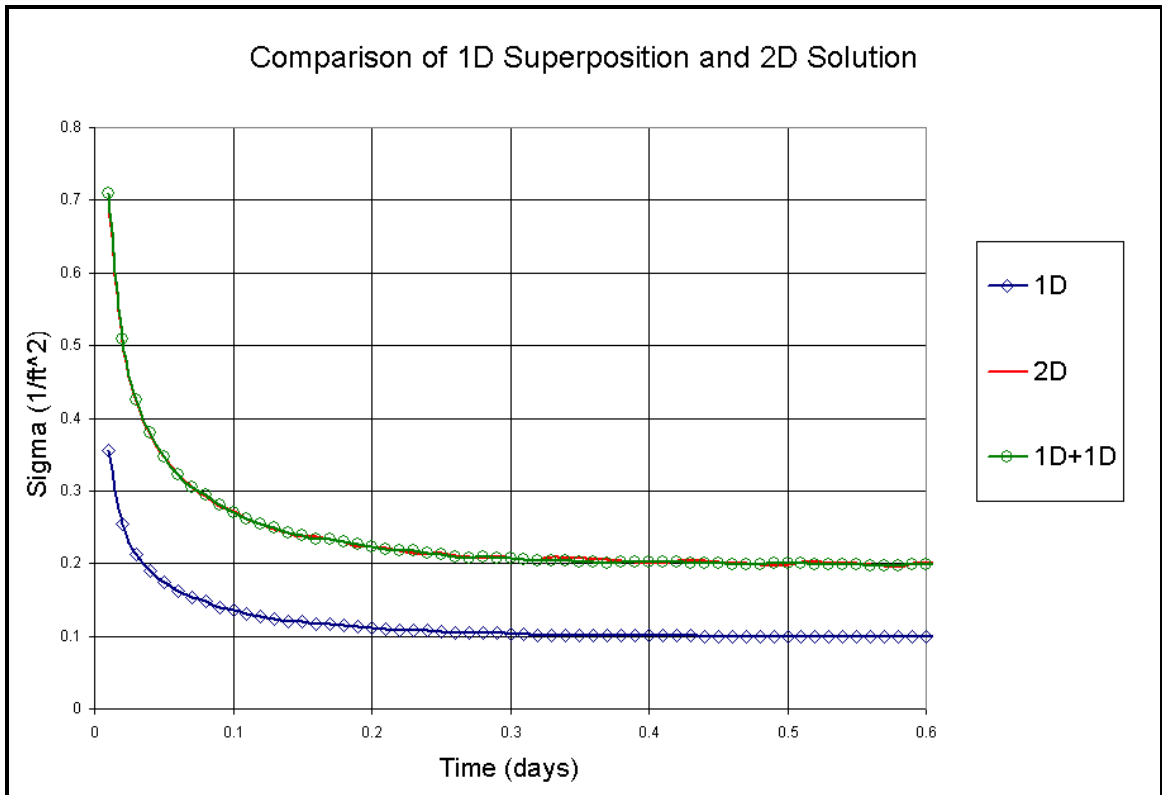


**Figure 3-12** Comparison of 1D superposition and 2D solution

We observe that the superposed 1D solution matches the real 2D solution exactly. Thus the applicability of superposition on the shape factor is verified. It is obvious that extension to 3D shape factors is trivial.

### 3.7. Validation and Comparison

In order to test the validity of the variable shape factor derived numerically, pressure drawdown behavior of the rhombic matrix-fracture system of Figure 3-10 is compared against its dual porosity counterpart, using the shape factor derived numerically as shown in Figure 3-11. Again, the system is initially at a constant pressure of 1000 psi, and the fracture pressure are suddenly reduced to 500 psi and maintained there.

The results of the comparison along with various other drawdowns obtained using constant pseudo-steady state factors are plotted in Figure 3-13.

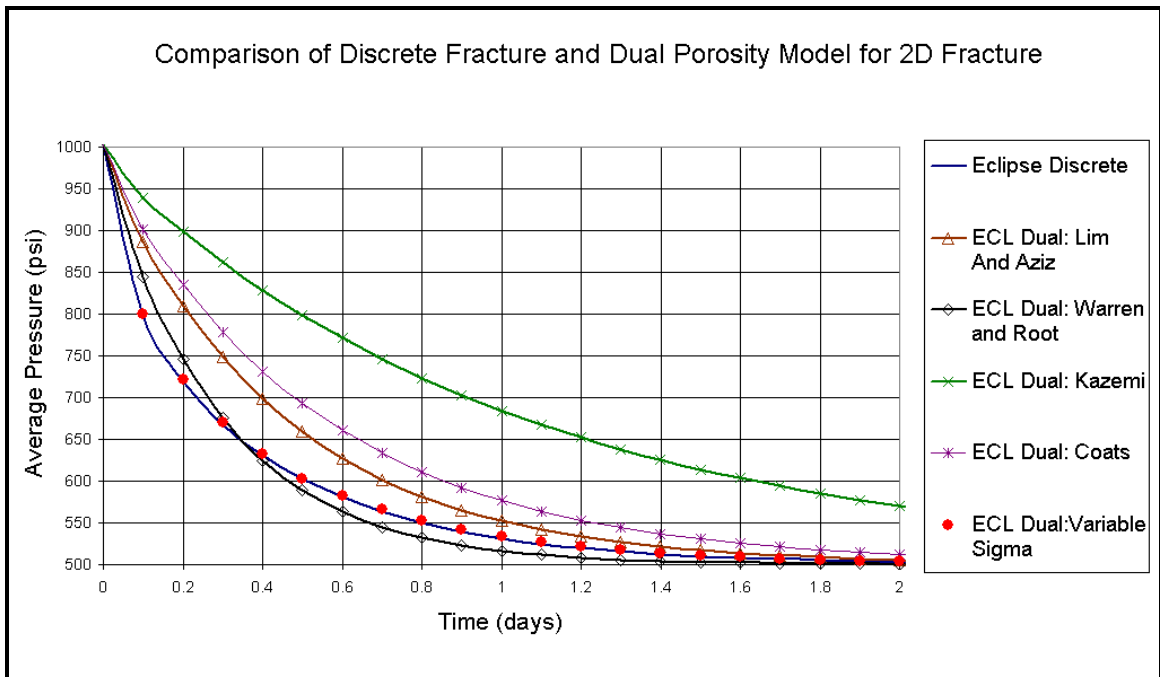


**Figure 3-13** Comparison of discrete fracture model and dual porosity models with different shape factors

The blue curve (without symbols) is the reference obtained directly from Matlab PDE Toolbox (MathWorks, 1996). The other curves are that obtained using a constant pseudo-steady state shape factor given by different researchers (Table 2-1), calculated for an

equivalent cubic system (equal volume as the rhombic matrix block). The red circles are obtained using the variable shape factor derived numerically. It is indeed clear the variable shape factor matches the reference almost exactly, verifying the validity of the proposed numerical technique.

The real benefit of the above technique is that it can just as easily be used to calculate the shape factors of very complex matrix shapes, and at the same time give both the transient and pseudo-steady state shape factors.

## **Chapter 4**

### **4 Two Phase Mass Transfer**

It has been shown in Chapter 2 that because of the existence of additional mechanisms in multiphase flow, a direct generalization of the single-phase transfer function is not applicable. In this chapter, mechanisms of two-phase mass transfer are first discussed and a complete definition of the transfer function in differential form applicable for two-phase as well as three-phase compressible flow is derived. It is then combined with the equations governing two-phase flow within the matrix block to arrive at a modified form of the transfer function for two-phase flow that accurately takes into account pressure diffusion (fluid expansion) and saturation diffusion (imbibition), which are the two main mechanisms driving two-phase flow. New shape factors for saturation diffusion are defined. Limitations of the current transfer function for multiphase flow are discussed, and it is shown that the prediction of wetting phase imbibition using the current transfer function is inaccurate, which might have significant consequences for reservoir management. Fine grid single porosity models are used again to verify the validity of the new transfer function. The results from single block dual porosity models and the corresponding single porosity fine grid models were in good agreement. Finally, implications of the new transfer function to reservoir management are discussed qualitatively.

#### **4.1. Mechanisms of Mass Transfer**

As has been discussed earlier, the gamut of mechanisms of mass transfer for a dual porosity media with multiphase flow include fluid expansion or pressure diffusion, imbibition or saturation diffusion, gravity imbibition or drainage, mass diffusion and viscous displacement or convection. Let us again use the conceptual model of a NFR as shown in Figure 4-1 to understand the importance of various mechanisms.

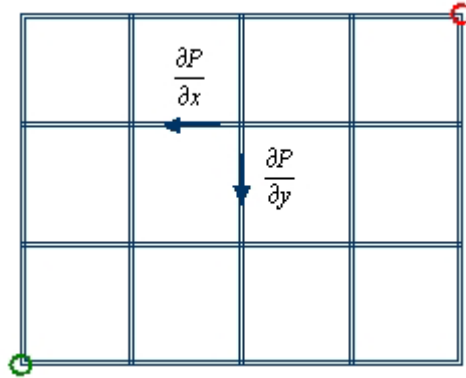


**Figure 4-1** Conceptual representation of a fractured reservoir with sources and sinks

With an argument similar to that made for single-phase flow, it can be shown that viscous displacement can be neglected for dual porosity mass transfer. With this assumption, the only forces left for multi-phase flow are fluid expansion (pressure diffusion), imbibition (saturation diffusion), gravity segregation and mass diffusion. Of these, the dominant forces for most NFRs are fluid expansion and imbibition. While gravity may in some cases play an important role, mass diffusion can be neglected. Hence, any transfer function defined for two-phase/multiphase flow would be accurate if it can take fluid expansion and imbibition into account accurately. The following derivation of the two-phase transfer function neglects gravity as a force of mass transfer, which is however accounted for later in the generalized model.

## 4.2. The Two Phase Transfer Function

Consider an arbitrary matrix block of volume  $V$  and porosity  $\phi$  surrounded by fractures on all sides. Oil and water present in the matrix and are assumed to be immiscible. At a time  $t$ , the average water saturation is  $\bar{S}_w$  and the average water density is  $\bar{\rho}_w$  in the matrix. The system is shown in Figure 4-2.

After a time  $dt$ , if the average saturation changes to  $\bar{S}_w + d\bar{S}_w$  and the average density to  $\bar{\rho}_w + d\bar{\rho}_w$ , then the change in the mass of water in the matrix is given as:

$$\begin{aligned}
&= V\phi(\bar{S}_w + d\bar{S}_w)(\bar{\rho}_w + d\bar{\rho}_w) - V\phi\bar{S}_w\bar{\rho}_w \\
&\square -V\phi\bar{S}_w d\bar{\rho}_w + V\phi\bar{\rho}_w d\bar{S}_w
\end{aligned} \tag{4.1}$$

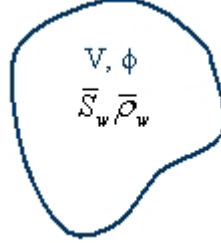


**Figure 4-2** An arbitrary matrix block with fractures on all sides

Therefore, the rate of matrix-fracture transfer of water:

$$q_{w_{mf}} = -V\phi\bar{S}_w \frac{\partial \bar{\rho}_w}{\partial t} + V\phi\bar{\rho}_w \frac{\partial \bar{S}_w}{\partial t} \tag{4.2}$$

Using the usual definition of compressibility (Aziz, 2001):

$$\frac{\partial \rho}{\partial t} = \rho c \frac{\partial p}{\partial t} \tag{4.3}$$

We have:

$$q_{w_{mf}} = -V\phi\bar{S}_w\bar{\rho}_w c_w \frac{\partial \bar{p}_w}{\partial t} + V\phi\bar{\rho}_w \frac{\partial \bar{S}_w}{\partial t} \tag{4.4}$$

$$q_{w_{mf}} = q_{w_{mf1}} + q_{w_{mf2}}$$

This is the complete differential form of the transfer function governing two-phase/multiphase flow in a matrix-fracture system. We need to calculate the two time

derivatives in the above equation in order come up with a transfer function that is simple and can be easily implemented in a reservoir simulator.

### 4.3. Limitations of Existing Models

Before we derive expressions for the two time derivatives, let us first understand the limitations of the existing transfer functions from a mathematical perspective. The complete transfer function, as we just derived, is given by Equation 4.4. However, we have already seen that the existing multiphase transfer function is a direct generalization of the single-phase transfer function. What it means is that the second part of Equation 4.4 is neglected in the existing transfer functions and the first part is modified to incorporate multiphase effects. Let us again look at the multiphase and single-phase transfer functions:

$$\begin{aligned}
 q_{w_{mf}} &= V \rho_w k \frac{k_{rw}}{\mu_w} \sigma(\bar{p}_w - p_{wf}) \\
 q_{mf} &= V \rho \frac{k}{\mu} \sigma(\bar{p} - p_f)
 \end{aligned}
 \tag{4.5}$$

We observe that the only difference between them is that the multiphase equation has an additional relative permeability term. Since we saw that the single-phase transfer only accounts for fluid expansion, this form of the multiphase transfer function is at best an approximation. Imbibition is modeled by use of capillary pressure curves without any physical justification. We will see later that this assumption is inaccurate for systems where both fluid expansion and imbibition are dominant, especially in modeling wetting phase imbibition rates.

### 4.4. Derivation of the Saturation Derivative

The differential form of the mass conservation equation gives us the complete equation governing mass transfer between a fracture and a matrix block (Aziz, 2001):

$$\sum_p \left\{ \nabla \omega_{c,p} \lambda_p (\nabla p_p - \gamma_p \nabla D) - \omega_{c,p} \tilde{q}_p^w - \frac{\partial}{\partial t} (\phi S_p \omega_{c,p}) \right\} = 0 \quad (4.6)$$

If we assume that oil and water are immiscible and the effect of gravity is ignored, and since we know that the effect of viscous forces (pressure differential) caused by sources and sinks on mass transfer between matrix and fracture is negligible, Equation 4.6 reduces to:

$$\nabla \rho_p \lambda_p \nabla p_p - \frac{\partial}{\partial t} (\phi S_p \rho_p) = 0 \quad (4.7)$$

Now,  $\rho_p$  is a function of pressure and  $\lambda_p$  is a function of saturation. Further, the functionality of  $\rho_p$  on pressure and  $\lambda_p$  on saturation cannot in general be defined analytically. Therefore, a useful and relevant assumption would be to consider them to be functions of average pressure and average saturation within the matrix block respectively. This assumption is relevant because the final difference form of the transfer function that we use within simulators calculates these parameters at the average pressures and saturations of the matrix. That is:

$$\rho_p(\bar{p}_p); \quad \lambda_p(\bar{S}_p) \quad (4.8)$$

Now, average pressure and average saturation within the matrix are independent of the spatial variables and only dependent on time, and therefore:

$$\rho_p(t); \quad \lambda_p(t) \quad (4.9)$$

Now, assuming that rock compressibility is constant, Equation 4.7 reduces to:

$$\nabla^2 p_p = \frac{\phi}{\lambda_p} \frac{\partial S_p}{\partial t} + \frac{\phi S_p c_p}{\lambda_p} \frac{\partial p_p}{\partial t} \quad (4.10)$$

Equations 4.10 for the oil-water system can be written as:

$$\begin{aligned}\nabla^2 p_w &= \frac{\phi}{\lambda_w} \frac{\partial S_w}{\partial t} + \frac{\phi S_w c_w}{\lambda_w} \frac{\partial p_w}{\partial t} \\ \nabla^2 p_o &= \frac{\phi}{\lambda_o} \frac{\partial S_o}{\partial t} + \frac{\phi S_o c_o}{\lambda_o} \frac{\partial p_o}{\partial t}\end{aligned}\tag{4.11}$$

Subtracting the water system from the oils system gives:

$$\nabla^2 (p_o - p_w) = \frac{\phi}{\lambda_o} \frac{\partial (1 - S_w)}{\partial t} - \frac{\phi}{\lambda_w} \frac{\partial S_w}{\partial t} + \frac{\phi S_o c_o}{\lambda_o} \frac{\partial p_o}{\partial t} - \frac{\phi S_w c_w}{\lambda_w} \frac{\partial p_w}{\partial t}\tag{4.12}$$

Replacing phase parameters in the last two terms by saturation weighted average parameters results in the following equation:

$$\nabla^2 P_c = -\phi \left[ \frac{1}{\lambda_o} + \frac{1}{\lambda_w} \right] \frac{\partial S_w}{\partial t} + \frac{\phi c_{av}}{\lambda_{av}} \frac{\partial P_c}{\partial t}\tag{4.13}$$

The average parameters are defined as:

$$f_{av} = \bar{S}_w f_w + \bar{S}_o f_o\tag{4.14}$$

We will see later that this assumption has no direct impact on the final result obtained.

We also have:

$$\nabla^2 P_c = \frac{dP_c}{dS_w} \nabla^2 S_w; \quad \frac{\partial P_c}{\partial t} = \frac{dP_c}{dS_w} \frac{\partial S_w}{\partial t}\tag{4.15}$$

Therefore Equation 4.13 reduces to:

$$\nabla^2 S_w = \left[ \frac{\phi c_{av}}{\lambda_{av}} - \phi \left( \frac{dP_c}{dS_w} \right)^{-1} \left\{ \frac{1}{\lambda_o} + \frac{1}{\lambda_w} \right\} \right] \frac{\partial S_w}{\partial t} \quad (4.16)$$

Again assuming that all parameters of the diffusivity of the above system are calculated at average pressure and saturation within matrix block, the hydraulic diffusivity of the above system is:

$$D(t) = \left[ \frac{\phi c_{av}}{\lambda_{av}} - \phi \left( \frac{d\bar{P}_c}{d\bar{S}_w} \right)^{-1} \left\{ \frac{1}{\lambda_o} + \frac{1}{\lambda_w} \right\} \right]^{-1} \quad (4.17)$$

Using the transform (Crank, 1975):

$$T = \int_0^t D(\tau) d\tau \quad (4.18)$$

We have the following Equation for saturation diffusion:

$$\frac{\partial S_w}{\partial T} = \nabla^2 S_w \quad (4.19)$$

A similar form of the water diffusion equation has been derived by Beckner et al. (1990) but with the assumption that  $\frac{\partial p_o}{\partial x} = \frac{\partial p_o}{\partial y} = 0$  and  $\vec{u}_o = -\vec{u}_w$ . This derivation does not involve any of the above assumptions. Note again that no assumptions about the shape of the matrix block, the boundary conditions or the initial conditions have been made to derive Equation 4.19.

For 1D imbibition of water in a matrix block from a fracture that is instantly filled with water (Rangel-German, 2002), the system can be written as:

$$\frac{\partial S_w}{\partial T} = \frac{\partial^2 S_w}{\partial x^2} \quad (4.20)$$

The boundary and initial conditions are (Rangel-German, 2002):

$$S_w(x, 0) = S_{wi}; \quad S_w(0, T) = S_{w\max} = S_{wf}; \quad S_w(\infty, T) = S_{wi} \quad (4.21)$$

Using the following dimensionless variables (Shaqfeh, 2001):

$$\theta = \frac{S_w - S_{wi}}{S_{wf} - S_{wi}}; \quad \eta = \frac{x}{2\sqrt{T}} \quad (4.22)$$

The solution to the above system is given as (Shaqfeh, 2001):

$$\theta(\eta) = \operatorname{erfc}(\eta) \square \frac{e^{-\eta^2}}{\sqrt{\pi\eta}} \quad (4.23)$$

The above approximation is valid for  $\eta > 2$  (Spiegel, 1999), which would be the case for usual reservoir parameters. We can now easily calculate volumetric average  $\theta$  for a matrix block of length L as follows:

$$\bar{\theta}(\eta_L) = \frac{1}{\eta_L} \left[ C_2 + \frac{1}{2\sqrt{\pi}} \operatorname{Ei}(\eta_L^2) \right] \quad (4.24)$$

Since we now have the average water saturation within the matrix block, we are in a position to obtain the saturation derivative:

$$\frac{\partial \bar{S}_w}{\partial t} = \frac{D(t)}{2 \int_0^t D(\tau) d\tau} (S_{wi} - \bar{S}_w) = \tilde{\sigma}_{SD} (S_{wi} - \bar{S}_w) \quad (4.25)$$

Here  $\tilde{\sigma}_{SD}$  is defined as the shape factor due to imbibition or saturation diffusion.

$$\tilde{\sigma}_{SD} = \frac{D(t)}{2 \int_0^t D(\tau) d\tau} \quad (4.26)$$

We can now calculate the second part of the transfer function:

$$q_{w_{mf}2} = V \phi \bar{\rho}_w \tilde{\sigma}_{SD} (S_{wi} - \bar{S}_w) \quad (4.27)$$

The shape factor given by Equation 4.26 can be reduced to a simplified form by realizing that it is a weak function of the hydraulic diffusivity  $D(t)$ , and in fact if  $D(t)$  is assumed constant, the shape factor reduces to:

$$\tilde{\sigma}_{SD} = \frac{1}{2} t^{-1} \quad (4.28)$$

We observe that this shape factor is a function of time similar to the transient shape factor.

#### 4.5. Derivation of the Pressure Derivative

The water system of Equation 4.10 can be rewritten as:

$$\frac{\partial p_w}{\partial t} = \frac{\lambda_w}{\phi S_w c_w} \nabla^2 p_w - \frac{1}{S_w c_w} \frac{\partial S_w}{\partial t} \quad (4.29)$$

To maintain consistency with previous assumptions, saturation  $S_w$  is replaced with average saturation  $\bar{S}_w$  within the matrix block. This assumption basically means that the diffusivity and the last term of the above equation (source term) are converted from time and space dependence to time dependence only, as was done before with mobility and density (Section 4.4). Thus we have:

$$\frac{\partial p_w}{\partial t} = \frac{\lambda_w}{\phi \bar{S}_w c_w} \nabla^2 p_w - \frac{1}{\bar{S}_w c_w} \frac{\partial \bar{S}_w}{\partial t} \quad (4.30)$$

Combining Equation 4.25 with Equation 4.30 we get:

$$\frac{\partial p_w}{\partial t} = \frac{\lambda_w}{\phi \bar{S}_w c_w} \nabla^2 p_w + \frac{\tilde{\sigma}_{SD}}{\bar{S}_w c_w} (\bar{S}_w - S_{wi}) \quad (4.31)$$

This can be rewritten as:

$$\frac{\partial p_w}{\partial t} = \alpha(t) \nabla^2 p_w + f(t) \quad (4.32)$$

The above equation is similar to the single-phase pressure diffusion equation used to calculate single-phase shape factors (Lim and Aziz, 1995) except for the presence of an additional source term  $f(t)$ . Further, we observe that hydraulic diffusivity is also a function of time and not constant. Thus applying the transform (Crank, 1975):

$$T = \int_0^t \alpha(\tau) d\tau \quad (4.33)$$

Equation 4.32 reduces to the following:

$$\frac{\partial p_w}{\partial T} = \nabla^2 p_w + \frac{f(t)}{\alpha(t)} \quad (4.34)$$

This can be rewritten as:

$$\frac{\partial p_w}{\partial T} = \nabla^2 p_w + \tilde{g}(T) \quad (4.35)$$

Here we have:

$$\tilde{g}(T) \equiv g(t) = f(t)/\alpha(t) \quad (4.36)$$

Equation 4.35 is exactly equivalent to the single-phase pressure diffusion equation in the sense that diffusivity in it is constant (equal to 1) but with an additional source term. Note that no assumptions have been made about the shape of the matrix block, the boundary conditions or the initial conditions to derive equation 4.35. Thus any solution of the single-phase pressure diffusion equation used to calculate single-phase shape factors would be applicable as a solution of Equation 4.35 but with an additional term representing the source term. For example, if we consider usual 1D mass transfer from a cubic matrix block to fractures on two opposite sides, with the system initially at a constant pressure and the fractures suddenly reduced and maintained at a constant pressure (same boundary conditions as used by Lim and Aziz, 1995), the system can be written as:

$$\frac{\partial p_w}{\partial T} = \frac{\partial^2 p_w}{\partial x^2} + \tilde{g}(T) \quad (4.37)$$

The boundary and initial condition are:

$$p_w(0, T) = p_w(L, T) = p_{wf} \quad (4.38)$$

$$p_w(x, 0) = p_{wm} \quad (4.39)$$

Using the following dimensionless variables:

$$P = \frac{p_w - p_{wf}}{p_{wm} - p_{wf}}; \quad \tau = \frac{T}{L^2}; \quad X = \frac{x}{L} \quad (4.40)$$

Equation 4.37 reduces to:

$$\frac{\partial P}{\partial \tau} = \frac{\partial^2 P}{\partial X^2} + \tilde{G}(\tau) \quad (4.41)$$

In the above equation:

$$\tilde{G}(\tau) \equiv \tilde{g}(T) = \frac{L^2 \tilde{g}(T)}{p_{wm} - p_{wf}} \quad (4.42)$$

The boundary and initial conditions are:

$$P(0, \tau) = P(1, \tau) = 0; \quad P(X, 0) = 1 \quad (4.43)$$

The solution of the above system can be found by the method of "Eigen Function Expansion" (Shaqfeh, 2001):

$$P(X, \tau) = \sum_{n=1}^{\infty} \left[ \int_0^t e^{n^2 \pi^2 \psi} c_n(\psi) d\psi + 2 \left( \frac{1 - \cos(n\pi)}{n\pi} \right) \right] e^{-n^2 \pi^2 \tau} \sin(n\pi X) \quad (4.44)$$

Here we have (Shaqfeh, 2001)::

$$c_n(\tau) = 2 \int_0^1 \tilde{G}(\tau) \sin(n\pi X) dX = 2 \left( \frac{1 - \cos(n\pi)}{n\pi} \right) \tilde{G}(\tau) \quad (4.45)$$

What we have to notice here is that the second term is the usual solution of the single-phase pressure diffusion for the same initial and boundary conditions (Lim and Aziz, 1995) and the first term is the extra term due to the presence of the source term. Thus the volumetric average pressure within the matrix block is derived as:

$$\bar{P}(\tau) = \sum_{n=1}^{\infty} \left( \frac{1 - \cos(n\pi)}{n\pi} \right) \left[ \int_0^t e^{n^2 \pi^2 \psi} c_n(\psi) d\psi + 2 \left( \frac{1 - \cos(n\pi)}{n\pi} \right) \right] e^{-n^2 \pi^2 \tau} \quad (4.46)$$

It has been shown that the above equation is very well approximated by the first term only for  $\tau > 0.1$  (Lim and Aziz, 1995), but which results in the pseudo-steady state assumption. For typical reservoirs that are slightly compressible, this time is equivalent to a few seconds. Thus we have:

$$\bar{P}(\tau) \approx \left[ \frac{2}{\pi} \int_0^t e^{\pi^2 \psi} c_1(\psi) d\psi + \frac{8}{\pi^2} \right] e^{-\pi^2 \tau} \quad (4.47)$$

$$c_1(\tau) = \frac{4}{\pi} \tilde{G}(\tau) \quad (4.48)$$

We can now calculate the required pressure derivative easily:

$$\frac{\partial \bar{p}_w}{\partial t} = -\sigma_{PD} \alpha(t) (\bar{p}_w - p_{wf}) + \frac{8}{\pi^2} \frac{\tilde{\sigma}_{SD}}{\bar{S}_w c_w} (\bar{S}_w - S_{wi}) \quad (4.49)$$

Here we have:

$$\sigma_{PD} = \frac{\pi^2}{L^2} \quad (4.50)$$

We can now derive the first part of the transfer function:

$$q_{w_{mf1}} = V \rho_w \lambda_w \sigma_{PD} (\bar{p}_w - p_{wf}) - V \phi \rho_w \frac{8}{\pi^2} \tilde{\sigma}_{SD} (\bar{S}_w - S_{wi}) \quad (4.51)$$

Equation 4.50 is the usual shape factor (Lim and Aziz, 1995, Chang, 1993) derived for single-phase pressure diffusion for two parallel fractures. We obtain the same shape factor because the pressure solution we obtain in Equation 4.44 is the same as that obtained by Lim and Aziz (1995) for the same boundary conditions, except for the presence of the new source term, which gives the second part of Equation 4.49 and 4.51. It is easy to

understand that  $\sigma_{PD}$  will always be the same as the single-phase shape factor of Lim and Aziz (1995) calculated for the same boundary conditions.

#### 4.6. Final Form of the Transfer Function

Combining Equation 4.4, 4.27 and 4.51, the complete transfer function can be written as:

$$q_{w_{mf}} = V \rho_w \lambda_w \sigma_{PD} (\bar{p}_w - p_{wf}) - V \phi \rho_w \left( \frac{8}{\pi^2} + 1 \right) \tilde{\sigma}_{SD} (\bar{S}_w - S_{wi}) \quad (4.52)$$

The constant in the second term can be absorbed into  $\sigma_{SD}$  to give:

$$q_{w_{mf}} = V \rho_w \lambda_w \sigma_{PD} (\bar{p}_w - p_{wf}) - V \phi \rho_w \sigma_{SD} (\bar{S}_w - S_{wi}) \quad (4.53)$$

For the particular case of two parallel fractures with pseudo-steady state pressure diffusion and instantaneously filled fractures, we obtained the following shape factors:

$$\begin{aligned} \sigma_{PD} &= \frac{\pi^2}{L^2} \\ \sigma_{SD} &= \left( \frac{8}{\pi^2} + 1 \right) \frac{D(t)}{2 \int_0^t D(\tau) d\tau} = bt^{-1} \end{aligned} \quad (4.54)$$

'b' is a constant in the above equation. As we saw, the first term is exactly equivalent to the usual single-phase transfer function. Thus we can easily generalize the above transfer function to accommodate any shape of the matrix and also transient pressure behavior, both of which would be represented by the shape factor  $\sigma_{PD}$ . A numerical algorithm was proposed in Section 3.6 to calculate this shape factor.

$$\begin{aligned} \sigma_{PD} &= \frac{a}{L^2} && \in \text{ Cubic Matrix and PSS (Lim and Aziz)} \\ \sigma_{PD} &= f(t) && \in \text{ Any shape and Tran + PSS (Numeric)} \end{aligned} \quad (4.55)$$

The second term is similar to the transfer function proposed by Rangel-German (2002) for incompressible imbibition that is given as:

$$\tau_{mf} = VD\sigma(S_{w\max} - \bar{S}_w) \quad (4.56)$$

The shape factor proposed by Rangel-German (2002) is given as:

$$\sigma = \sigma^* \left( \frac{t_D}{t_D^*} \right)^{-m} \quad \in t_D < t_D^* \quad (4.57)$$

$$\sigma = \sigma^* \quad \in t_D > t_D^* \quad (4.58)$$

This shape factor initially decreases with time (effect of filling-fracture regime) and then becomes constant and equal to the pseudo-steady state shape factor. This result is based on experimental results and dimensional analysis. The condition  $\sigma = \sigma^*$  for  $t_D > t_D^*$  is imposed in order that the transfer function can account for pseudo-steady state flow.

The transfer function derived here separates the effects of capillary imbibition and pseudo-steady state flow into two different transfer functions. Thus,  $\sigma_{SD}$  decreases with time continuously and  $\sigma_{PD}$  becomes constant and equal to the pseudo-steady state shape factor. In combination, the final mass transfer through this approach should be similar to that given by Rangel-German (2002). However, the transfer function and shape factor described here were obtained mathematically and that defined by Rangel-German (2002) are based only on experiments and dimensionless analysis. One limitation of Rangel-German's (2002) transfer function is that it cannot be used for single-phase flow. Further the factor 'm' has to be derived experimentally.

In order to incorporate the affect of the "filling-fracture" regime into  $\sigma_{SD}$ , let us compare it to Rangel-German's (2002) shape factor that accounts for the "filling-fracture" regime. For constant diffusivity, we saw that  $\sigma_{SD}$  reduces to:

$$\sigma_{SD} = bt^{-1} \quad (4.59)$$

This has been derived for the “instantly-filled” fracture regime. Here  $b$  is a constant given by Equation 4.54.

As shown before, the shape factor proposed by Rangel-German (2002) is given as:

$$\sigma = \sigma^* \left( \frac{t_D}{t_D^*} \right)^{-m} \quad (4.60)$$

Thus, in order to incorporate the affect of the “filling-fracture” regime into  $\sigma_{SD}$ , a direct generalization is suggested by comparing Equation 4.59 and Equation. 4.60:

$$\begin{aligned} \sigma_{SD} = bt^{-1} & \quad \in \text{ Instantly filled fracture} \\ \sigma_{SD} = bt^{-m} & \quad \in \text{ Gradually filling fracture} \end{aligned} \quad (4.61)$$

As suggested by Rangel-German (2002), ‘ $m$ ’ is a function of flow rate and fracture aperture, in other words, a function of the rate of propagation of water in the fracture. ‘ $b$ ’ and ‘ $m$ ’ can be determined through optimization against experimental results or fine grid simulation.

## 4.7. Validation and Comparison

The proposed transfer function is validated for a single matrix block model undergoing two-phase compressible flow. The system is such that both fluid expansion and imbibition are important forces driving mass transfer. Figure 4-3 depicts the conceptual model.

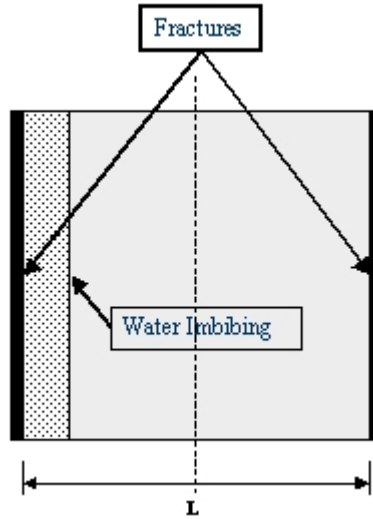


**Figure 4-3** Cubic matrix with two fractures, with imbibition through one fracture

The properties of the system are as under:

Dimens: 200X200X200 cu. ft.	Fracture Pressure: 500 psi
Porosity: 5%	Capillary Pressure: < 100 psi
Matrix Perm: 1 md	Compressibility: 0.0001 /psi
Fracture Perm: 10 d	Initial Water Saturation: 0.2
Initial Pressure: 1000 psi	Relative Perm: Corey Type

**Table 4-1** Properties of the validation model

The system is placed on a pressure drawdown through the two fractures by reducing their pressures to 500 psi, and simultaneously water is introduced into one of the fractures. The system is set up in such a way that the fractures fill up instantaneously with water. The new transfer function is validated against a fine grid model (ECLIPSE 100). Figure 4-4 and 4-5 show the variation of the saturation and pressure fields within the matrix block. We see that pressure is reducing from both fractures and water is imbibing through one fracture.

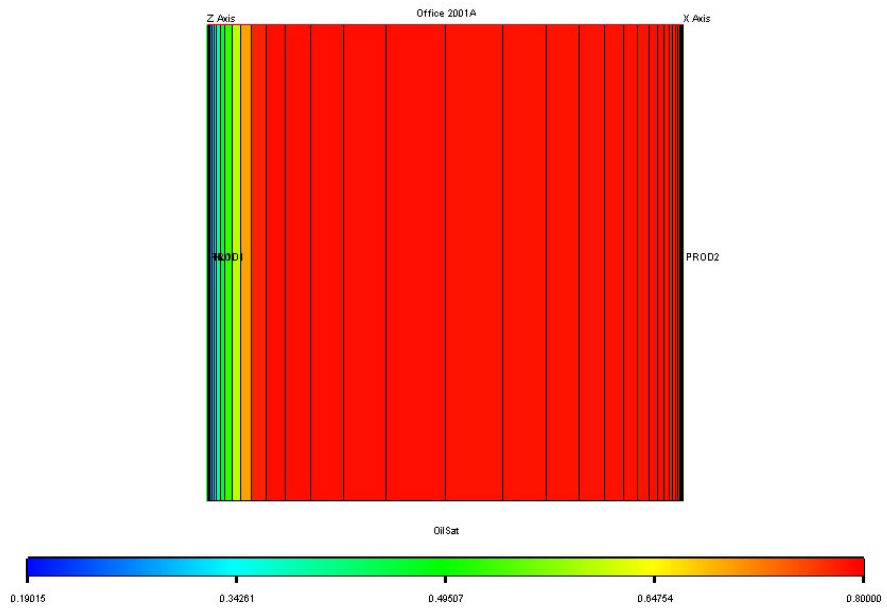


**Figure 4-4** Saturation profile at 20 days

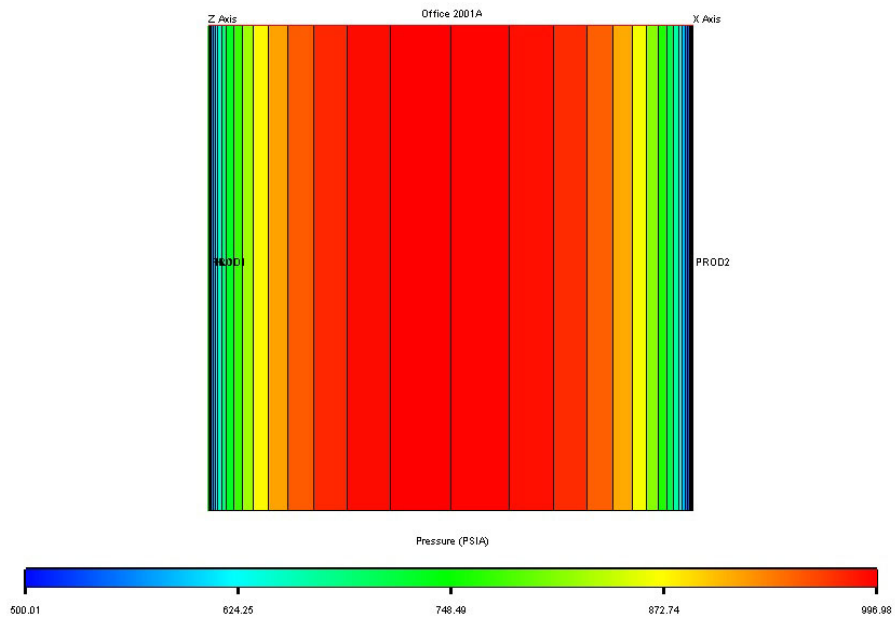


**Figure 4-5** Pressure profile at 1 day

Figure 4-6 compares the oil production rate from the matrix block for the fine grid model, the new transfer function and the current transfer function (ECLIPSE 100 Dual Porosity Model) with shape factors of Lim and Aziz (1995). The green curve (with crosses) is the reference solution from the fine grid model, the blue curve (with rhomboids) from the new transfer function and the red one (with circles) from the current transfer function, i.e., only the first term of the complete transfer function. It is obvious that the new transfer function does a better job of modeling the oil production rate. However, the real significance of the new transfer function can be seen from comparison of the water imbibition rates into the matrix block, which is shown in Figure 4-7.

Here again, the green curve (with crosses) is the reference, the blue curve (with rhomboids) is using the complete transfer function and the red one (with circles) from the current transfer function. We observe that the match with the complete transfer function is not as good as for the oil rate, but on the whole the form of the curve is maintained and at late time matches the true solution exactly. But the current transfer function completely fails to model the water imbibition rates. When the rate should be maximum it is actually zero, and when it should be decreasing it is increasing.

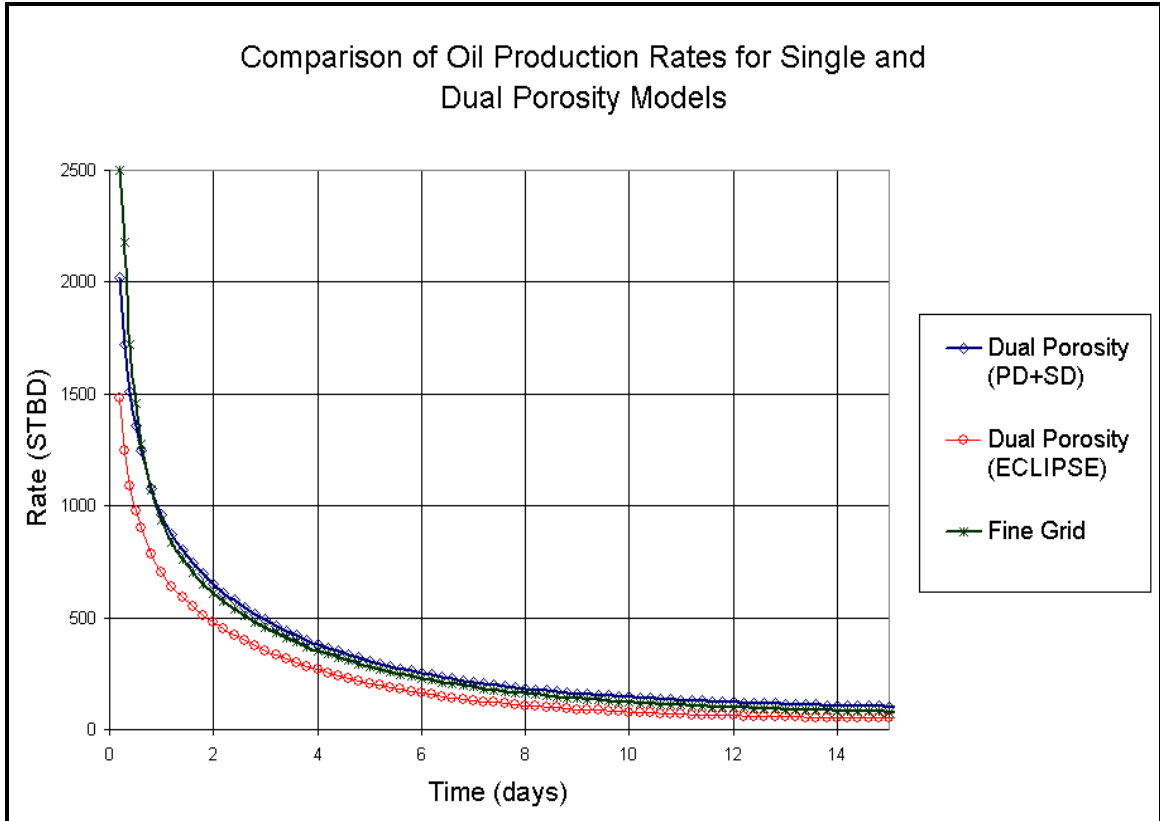


**Figure 4-6** Comparison of oil production rates for  $m = 1.06$

There is a physical explanation as to why the current transfer function completely fails to model wetting phase imbibition. Figure 4-8 shows the average oil (green curve) and water (light blue curve) pressures in the matrix, the fracture pressure (dark blue, same for both oil and water as fracture  $P_c = 0$ ), and the water imbibition rate. We see that initially up to around 5 days, water pressure in the matrix block is above the fracture pressure. Thus, with the current transfer function, due to upstream weighting, the upstream side would be calculated as the matrix block, and since initially there is only connate water in the matrix block, its relative permeability is zero. Thus the water mobility is zero for the current transfer function, and thus the water imbibition rate is zero. Only when the matrix water pressure reduces below the fracture pressure does the upstream direction change, which in turn allows water to imbibe.

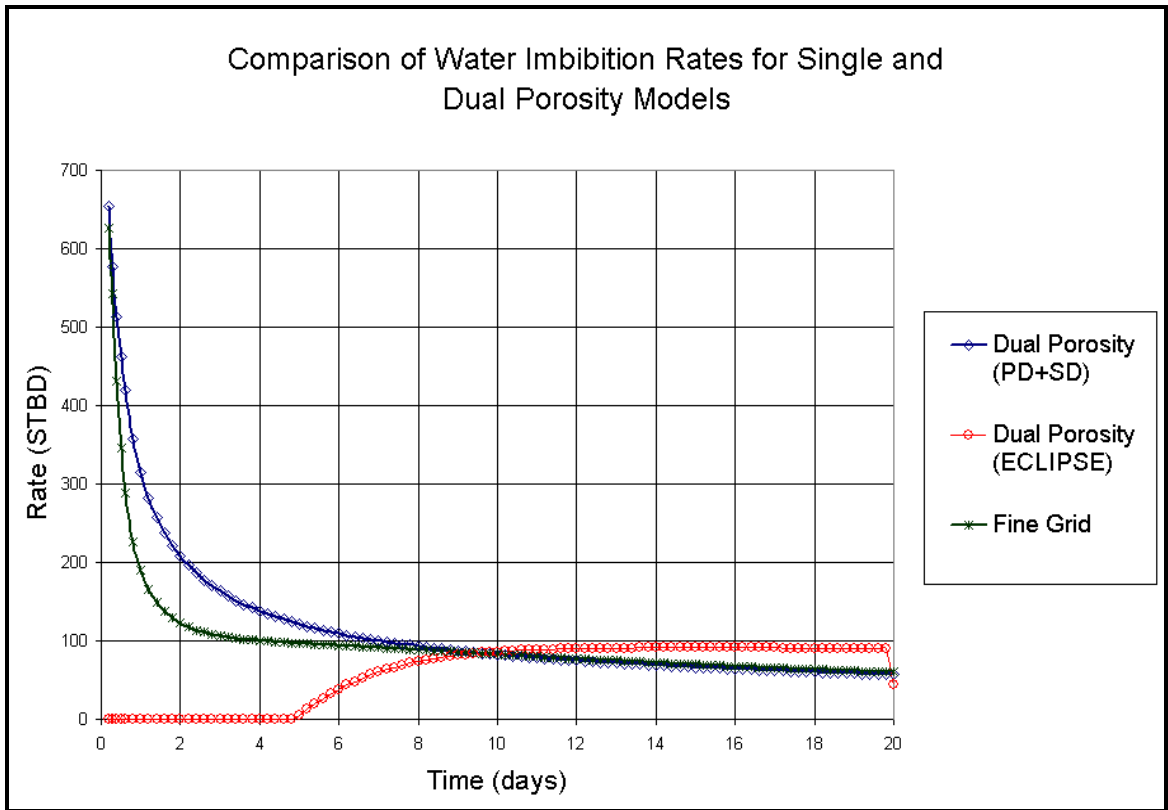


**Figure 4-7** Comparison of water imbibition rates for  $m = 1.06$

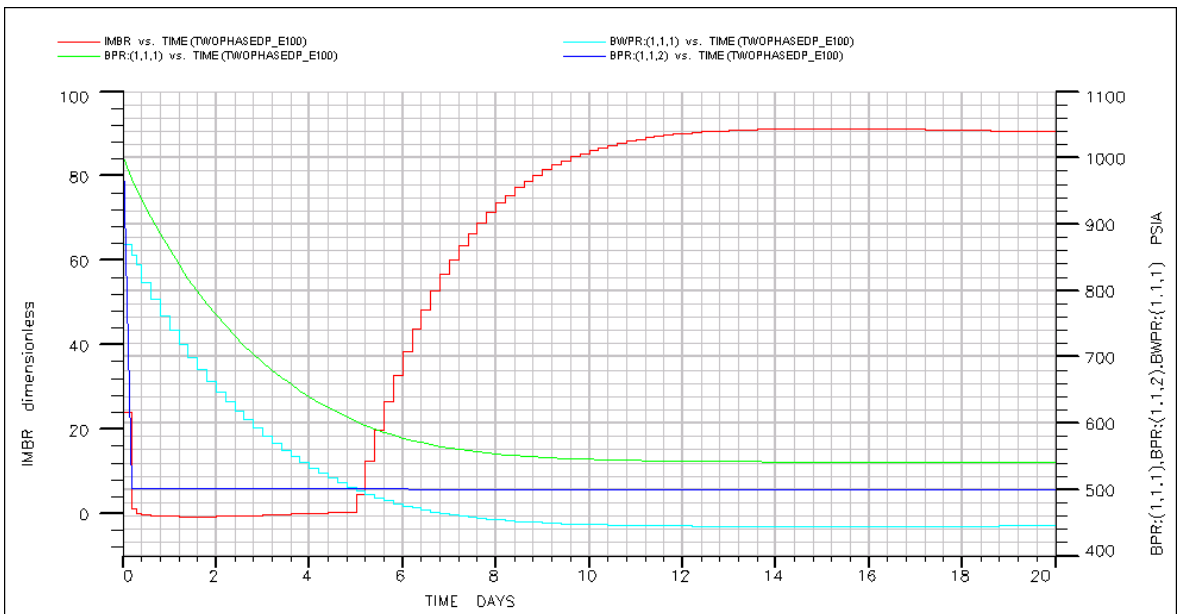


**Figure 4-8** Explanation of 0 initial imbibition rate for current transfer function

It is easily seen that this phenomenon will always occur whenever there is imbibition in a compressible dual porosity system. Thomas et al. (1983) understood this phenomenon and used a scheme of weighted average mobilities of the upstream and downstream sides to correct this discrepancy. However, as already mentioned, although such a scheme can help correct the discrepancy, it is non-physical since the equations governing saturation transport are hyperbolic, meaning that only upstream properties govern transport.

This phenomenon might have significant consequences to reservoir management of NFRs, specifically NFRs undergoing waterfloods. We have observed that the initial water imbibition rates given by the current transfer function is much lower compared to the reference solution. Thus, with the existing transfer function, whenever new matrix blocks come in contact with injected water, the predicted imbibition rates would be much lower than the true rates, which should result in an early prediction of water breakthrough time. Breakthrough time is a very important parameter affecting the economics of waterfloods projects, and therefore its accurate prediction is essential. The use of the new transfer function might help in a more accurate prediction of breakthrough time. Further, it should also give a better prediction of production rates and recoveries. However, establishing the significance of using the new transfer function requires field scale studies.

## Chapter 5

### 5 Extensions to Three Phase Compositional Flow

We have in the last chapter developed a new transfer function for two phase immiscible flow that accurately described the mechanisms of fluid expansion and imbibition. It was also shown that the form of the transfer function itself is different for single-phase and two-phase flow, the reason being that for single-phase flow, the only mechanism present was fluid expansion, but for two-phase flow, additional mechanisms of imbibition and gravity segregation existed. However, the addition of a third phase does not introduce new flow governing mechanisms. Also, the differential form of the transfer function derived in Section 4.2 is applicable to three-phase flow as well. Thus, it is obvious that the development of the last chapter can be directly generalized to three-phase flow.

This understanding, together with the dual porosity/dual permeability formulation for multiphase compositional flow discussed in Section 2.4 on the current dual porosity/dual permeability model, gives us the finite difference form of the matrix-fracture equations for a control volume with 'ns' surfaces as below:

$$\left\{ \left[ \sum_{s=1}^{ns} [T_s \sum_p (\lambda_p \rho_p X_{cp} \Delta \Phi_p)_s] + WI^W \cdot \sum_p [\lambda_p \rho_p X_{cp} (p_p - p^W)] \right]^{n,n+1} \right\}_m - \tau_{c_{mf}} = \left\{ V \frac{\phi^{n+1} \sum_p (S_p \rho_p X_{cp})^{n+1} - \phi^n \sum_p (S_p \rho_p X_{cp})^n}{\Delta t} \right\}_m \quad (5.1)$$

$$\left\{ \left[ \sum_{s=1}^{ns} [T_s \sum_p (\lambda_p \rho_p X_{cp} \Delta \Phi_p)_s] + WI^W \cdot \sum_p [\lambda_p \rho_p X_{cp} (p_p - p^W)] \right]^{n,n+1} \right\}_f + \tau_{c_{mf}} = \left\{ V \frac{\phi^{n+1} \sum_p (S_p \rho_p X_{cp})^{n+1} - \phi^n \sum_p (S_p \rho_p X_{cp})^n}{\Delta t} \right\}_f \quad (5.2)$$

Again, the RHS is the accumulation part, the first term on the LHS is the flux through all the surfaces of the control volume and the second term on the LHS is the well flux. However,  $\tau_{c_{mf}}$  now represents the new transfer function.

If the matrix and matrix block face pressures can be approximated by their values at grid nodes (Aziz, 2001), then, the new transfer function for multiphase compositional flow is given as:

$$\tau_{c_{mf}} = V k_m \sigma_{PD} \sum_p \left[ \lambda_p \rho_p X_{cp} (\Phi_{pm} - \Phi_{pf}) \right] - V \phi_m \sigma_{SD} \sum_p \left[ \rho_p X_{cp} (S_p - S_{pi}) \right] \quad (5.3)$$

Here,  $\Phi$  is the total potential that includes the pressure potential and gravity potential, and is usually equal to the potential given by Kazemi et al. (Equation 2.7) or Litvak (Equation 2.13). However, it should be understood again that the above treatment of gravity inherently assumes that a linear superposition of gravity segregation, fluid expansion and imbibition is applicable (Fung, 1993). In other words, it is assumed that gravity acts as a force that just separates the fluids without directly "affecting" the process of fluid expansion or imbibition. Further, it is also assumed that the fluids are completely segregated within the matrix block. A more rigorous incorporation of gravity would be desirable.

## Chapter 6

### 6 Implementation into GPRS

GPRS is an acronym for “General Purpose Research Simulator” developed at Stanford University (Cao, 2002). One of the main purposes behind its development was to create a flexible simulation test bench where new models can be easily and quickly implemented. This not only helps researchers to quickly test new ideas and preserve their work under a standard roof, but also makes it possible for future investigators to easily extend on them. This chapter discusses the implementation of the proposed dual porosity/dual permeability model into GPRS and its validation. Due to the modular object oriented approach in the design of GPRS, modifications of GPRS to accommodate the proposed dual porosity/dual permeability model are relatively straightforward. The implementation is done in such a way that it causes minimum “friction” with the existing code, is structured and organized, and on the whole maintains the object oriented nature of the original code.

#### 6.1. Modifications to Formulation

The control volume compositional formulation implemented in GPRS is as follows (Cao, 2002):

$$\begin{aligned} & V \frac{\phi^{n+1} \sum_p (S_p \rho_p X_{cp})^{n+1} - \phi^n \sum_p (S_p \rho_p X_{cp})^n}{\Delta t} \\ & = \left\{ \sum_{s=1}^{ns} [T_s \sum_p (\lambda_p \rho_p X_{cp} \Delta \Phi_p)_s] + WI^W \cdot \sum_p [\lambda_p \rho_p X_{cp} (p_p - p^W)] \right\}^{n,n+1} \end{aligned} \quad (6.1)$$

Here, the LHS is the accumulation part, the first term on the RHS is the flux through all the surfaces of the control volume and the last term on the RHS is the well flux. As we

saw before, for a dual porosity/dual permeability model, two sets of equations very similar to the above are required, one for the matrix system and one for the fracture system.

$$\left\{ \left\{ \sum_{s=1}^{ns} [T_s \sum_p (\lambda_p \rho_p X_{cp} \Delta \Phi_p)_s] + WI^W \cdot \sum_p [\lambda_p \rho_p X_{cp} (p_p - p^W)] \right\}^{n,n+1} \right\}_m - \tau_{c_{mf}} = \left\{ V \frac{\phi^{n+1} \sum_p (S_p \rho_p X_{cp})^{n+1} - \phi^n \sum_p (S_p \rho_p X_{cp})^n}{\Delta t} \right\}_m \quad (6.2)$$

$$\left\{ \left\{ \sum_{s=1}^{ns} [T_s \sum_p (\lambda_p \rho_p X_{cp} \Delta \Phi_p)_s] + WI^W \cdot \sum_p [\lambda_p \rho_p X_{cp} (p_p - p^W)] \right\}^{n,n+1} \right\}_f + \tau_{c_{mf}} = \left\{ V \frac{\phi^{n+1} \sum_p (S_p \rho_p X_{cp})^{n+1} - \phi^n \sum_p (S_p \rho_p X_{cp})^n}{\Delta t} \right\}_f \quad (6.3)$$

Here, the additional term  $\tau_{c_{mf}}$  is the transfer function that controls fluid transfer between and fracture block and the connected matrix block. If the matrix and matrix block face pressures can be approximated by their values at grid nodes (Aziz, 2001), then:

$$\tau_{c_{mf}} = V k_m \sigma_{PD} \sum_p [\lambda_p \rho_p X_{cp} (\Phi_{pm} - \Phi_{pf})] - V \phi_m \sigma_{SD} \sum_p [\rho_p X_{cp} (S_p - S_{pi})] \quad (6.4)$$

To model such systems, two simulation cells are associated with each block in the geometric grid, representing the matrix and fracture volumes of the cell. Therefore, for a dual porosity/dual permeability run, the number of layers in the Z (NZ) direction has to be doubled (and therefore even). The first half of the layers (1 to NZ/2) will be associated with the matrix blocks and the second half (NZ/2 + 1 to NZ) will be associated to the fracture blocks (Eclipse 100 Technical Description, 2000).

Thus the first modification necessary in GPRS is to the gridding module that calculates the cell list and connection list. There can be two approaches to the tackle above problem.

In the first, if the internal grid generation module of GPRS is used, this can be handled quite easily by just increasing the number of grids to twice in the Z direction and populating the top half layers with matrix properties and the bottom half layers with fracture properties. An additional module to remove connections between the  $NZ/2$  and  $NZ/2+1$  layers has to be implemented, which is clearly not physical; but which would otherwise be included in the output of the existing gridding algorithm. This is explained in later sections.

The second approach is to use external gridding software, which would clearly be necessary for realistic NFRs. Characterization of any realistic NFR would lead to two geostatistical models, one for the matrix continuum and one for the fracture system. Thus the physical simulation grid created by any gridding software has to be once populated by the matrix system properties and once by the fracture system properties. This would result in two cell lists and two connection lists, the cell and connection numbers being the same in both lists, but the properties associated with the same cell (volume, porosity) and same connection (transmissibility constant) would be different for the two sets. Thus a module has to be written that will combine both cell lists into one and both connection lists into one. This will be discussed in detail later.

The second and main modification is related to the formulation of the residual vector and the jacobian matrix. The jacobian matrix is generated by calculating the derivatives of Equation 6.2 and 6.3 with respect to all of the unknowns (variables). In GPRS, the jacobian matrix is calculated and stored separately for the reservoir part (accumulation, flux and dual porosity transfer terms) and for the well part, and it is later pieced together only in the linear solver module (Cao, 2002). Only the reservoir part of the jacobian matrix needs to be modified. Thus the well part will not be discussed here.

The structure of the reservoir part of the jacobian is shown in Figure 6-1. It consists of three arrays, **Diag**, **OffD\_A** and **OffD\_B**. **Diag** is the diagonal part, each of its entries is for one gridblock, and the location of each entry follows the cell list. **OffD\_A** records the

sparse structure of the upper triangular part, and **OffD\_B** records the sparse structure of the lower triangular part. Each of their entries is for one connection, and the location of each entry follows the connection list. For example, for a connection between gridblock A and B ( $A < B$ ), **OffD\_A** stores the derivative of equations of gridblock A with respect to variables of gridblock B, and it is located at (A, B) of the jacobian matrix. Similarly **OffD\_B** at (B, A) contains the derivatives of equations of gridblock B with respect to variables of gridblock A. For multi-point flux, **OffD\_A** and **OffD\_B** will include more entries. For jacobian calculations of the reservoir part, the accumulation part, dual porosity transfer part and the flux part are further separated. The accumulation part loops through the cell list, and it only adds terms in the **Diag** array; the flux part loops through the connection list, and it contributes to all three arrays. For multi-component system, each of the entries in these arrays is a small dense matrix (Cao ,2002).

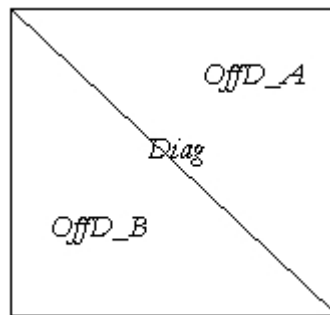


**Figure 6-1** Structure of reservoir part of jacobian (Cao, 2002)

Now consider the dual porosity transfer term in Equation 6.2 and 6.3. It has certain characteristics similar to the accumulation term and some to the flux term. The similarity to the accumulation term is that there is one dual porosity transfer term in each equation just like the accumulation term, i.e., one term per gridblock per component. This necessitates the dual porosity transfer term to loop through the cell list. The similarity to the flux term is that it is also a flux, though not with neighboring gridblocks, but with a matrix or fracture block at a distance of  $N$  ( $2N = \text{total gridblocks}$ ) from it on the cell list. Also, the dual porosity transfer term contains variables of both the matrix and the fracture grids, and thus would contribute to both diagonal and off-diagonal parts of the

jacobian. However the number of flux terms per equation depends on the number of surfaces or connections, unlike the dual porosity term that is only one. Further, there is no explicit connection list for the dual porosity transfer term, as the connections are always implicitly defined as between any matrix block 'i' and a fracture block 'i+N'. Even more importantly, the dual porosity transfer term is calculated differently as compared to a flux term. Thus, with these insights, the best way to calculate the dual porosity terms is to loop through cell list, but this part adds terms to the **Diag** array, and to two new arrays, **DPOffD\_A** and **DPOffD\_B**. Because of the above-mentioned differences between flux terms and the dual porosity transfer term, **OffD\_A** and **OffD\_B** cannot be used to store the off-diagonal parts of the transfer term. This use of new arrays creates a few complexities and does not keep the code completely modular. However, this is inevitable given the design of GPRS. Thus, the new structure of the jacobian is given as:

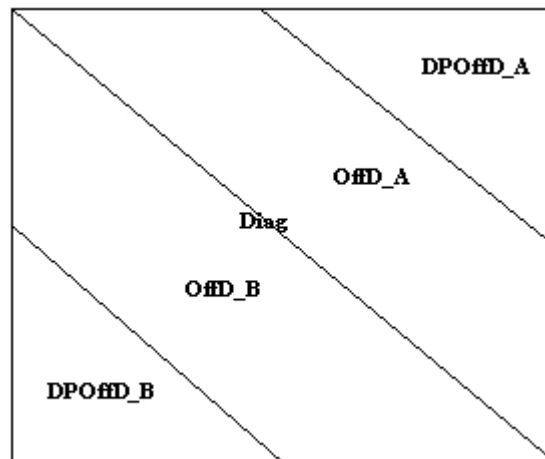


**Figure 6-2** New structure of jacobian

The complexities that arise due to use of new arrays are fourfold, three of which are related to the General Formulation Approach (Cao, 2002). There are essentially the three main steps in this approach. The first is switching variables from Type A (natural variables) to Type B, if necessary. The second is to reduce the full set of equations to the primary set, which is only required for the compositional formulation. The third is to further reduce the implicit level if necessary. All the manipulations that are done on

OffD\_A and OffD\_B in this process are also required on DPOffD\_A and DPOffD\_B. The last is related to the solver classes, to which the new arrays have to be passed as well and there rearranged to a form acceptable to the linear solver. This has a disadvantage in that it results in a loss of modularity of the code. However, the object-orientedness can be maintained through proper use of C++ coding concepts.

In order to make the structure of the jacobian matrix clearer, a simple two-well two-layer example is included here. The grid is shown in Figure 6-3. Well 1 is completed in gridblocks 8 and 9 in the fracture system, and well 2 is completed in gridblocks 12. The corresponding jacobian matrix for this system is shown in Figure 6-4, where "A" represents a term generated by the accumulation part, "F" represents a term generated by the flux part, "D" represents a term generated by the dual porosity part and "W" represented a term generated by the well part.

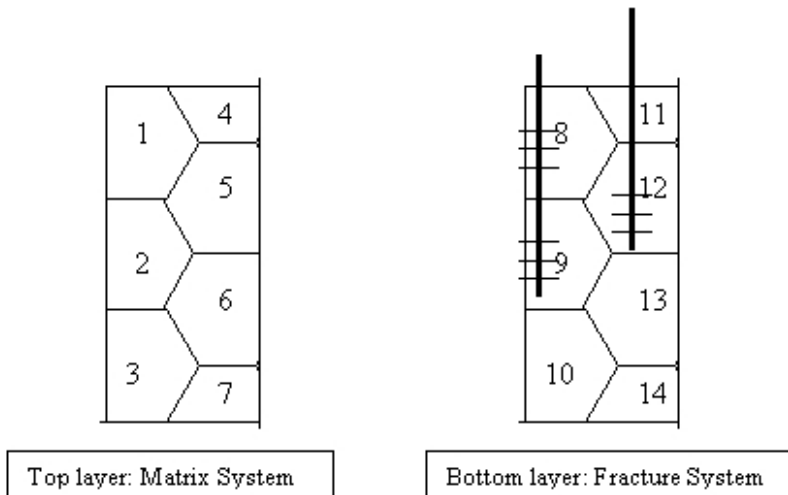


**Figure 6-3** Simple NFR with two wells completed in fracture system

The procedure for calculation of the reservoir part of the jacobian matrix and residual calculation using this Cao's (2002) connection based approach is slightly modified to accommodate the dual porosity term as follows:

First, loop through the cell list, and evaluate the accumulation terms and their derivatives for each gridblock. The accumulation terms are assigned to the residual, and the derivatives are assigned to the diagonal of the jacobian matrix at the corresponding

gridblocks. Also during the same loop, and only for the first half of the cell list (i.e., the matrix blocks), calculate the dual porosity transfer term DP from matrix gridblock 'm' to fracture block 'f'. If 'i' is the index of the matrix block in the cell list, then the fracture block has an index of 'i'+N (2N = total grid blocks). Assign -DP to the residual term in the residual vector corresponding to the matrix block and DP to the residual term for the fracture block. If Xm and Xf are the variables for the matrix gridblock and the fracture block, calculate  $\frac{\partial DP}{\partial X_m}$  and  $\frac{\partial DP}{\partial X_f} \cdot \frac{\partial DP}{\partial X_m}$  and  $-\frac{\partial DP}{\partial X_f}$  are stored in **Diag**, corresponding to the matrix and fracture block respectively, and  $\frac{\partial DP}{\partial X_f}$  is stored in **DPOffD\_A** and  $-\frac{\partial DP}{\partial X_m}$  is stored in **DPOffD\_B**, as shown in Figure 6-5.

	1	2	3	4	5	6	7	8	9	10	11	12	13	14	W1	W2
1	AFD	F		F	F			D								
2	F	AFD	F		F	F			D							
3		F	AFD			F	F			D						
4	F			AFD	F						D					
5	F	F		F	AFD							D				
6		F	F		F	AFD	F						D			
7			F			F	AFD							D		
8	D							AFD	W	F	F	F	F		W	
9		D						F	AFD	W	F	F	F		W	
10			D						F	AFD		F	F			
11				D				F			AFD	F				
12					D			F	F		F	AFD	W	F		W
13						D			F	F		F	AFD	F		
14							D			F			F	AFD		
W1								W	W						W	
W2												W				W

**Figure 6-4** Structure of jacobian for the above reservoir

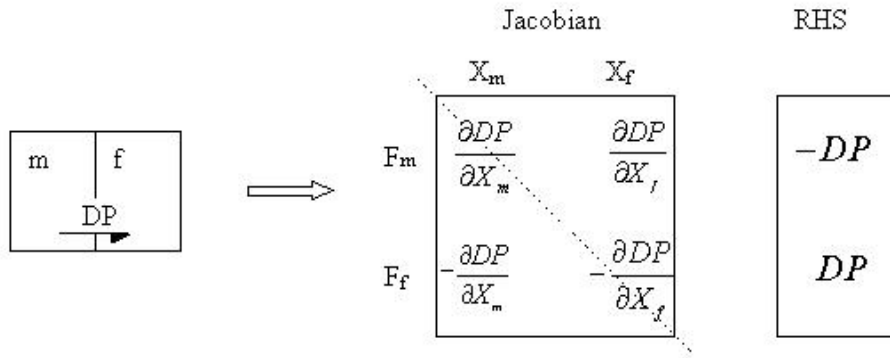


**Figure 6-5** jacobian structure for Dual Porosity transfer derivatives

Next, loop through the connection list, calculate the upstream direction for each phase and evaluate the flux terms and their derivatives for each connection. The flux terms are added to the residual of the connected blocks, one is positive and the other is negative, the derivatives are added to the correct locations in the jacobian matrix, as shown in Figure 6.6 for a two-point flux calculation. Flux  $F_{AB}$  is from gridblock A to gridblock B,  $X_A$  and  $X_B$  are the variables at gridblock A and B, and  $F_A$  and  $F_B$  are the equations at gridblock A and B.  $\frac{\partial F_{AB}}{\partial X_A}$  and  $-\frac{\partial F_{AB}}{\partial X_B}$  are stored in **Diag**, and  $\frac{\partial F_{AB}}{\partial X_B}$  is stored in **OffD\_A**, and  $-\frac{\partial F_{AB}}{\partial X_A}$  is stored in **OffD\_B**.

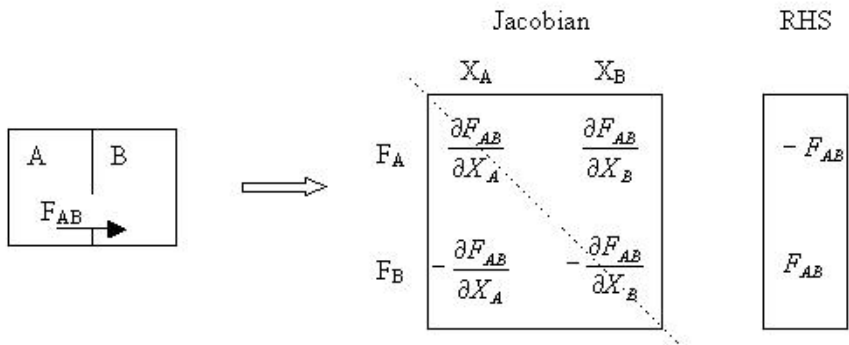


**Figure 6-6** jacobian structure for 2-point flux derivatives

This modification applies directly to multipoint flux calculations as well.

## 6.2. Modifications to Design

Modifications related to the design aspects of GPRS can be best understood through system model diagrams given by Cao (2002). The basis of all modifications are the concepts of Inheritance and Polymorphism (Deitel et al., 1998), which are used in order that the least possible number of changes be made to the existing code, and at the same time maintaining the object-oriented nature of the code. The philosophy behind the ideas of Inheritance and Polymorphism is that, rather than directly make changes to existing code, create new classes as extensions to existing classes, and make all necessary changes in these new classes (Deitel et al., 1998). This process helps in keeping the changes in the existing code to a minimum. This has many benefits in the sense that the code so produced is more organized with new modules kept completely separate from existing modules. Further, this makes possible the reuse of already existing debugged software, reducing the possibility of logical errors.

The domain level system model is shown in Figure 6.7. Each domain includes a reservoir and several wells. Besides that, each domain also has an Equation Selector module and a Linear Solver module. In GPRS, the jacobian matrices are calculated separately for the reservoir part and for the well part, the Equation Selector module is used to recast the jacobian with desired variables and implicit levels. After that the jacobian matrices are passed to the Linear Solver and pieced together there for the linear solve. Finally, the solution goes back in the opposite direction. Most of the major modifications necessary to implement the dual porosity/dual permeability model will be in the Reservoir Module marked in red (top left block). As mentioned before, some changes are also required in the Equation Selector classes and the Linear Solver classes.

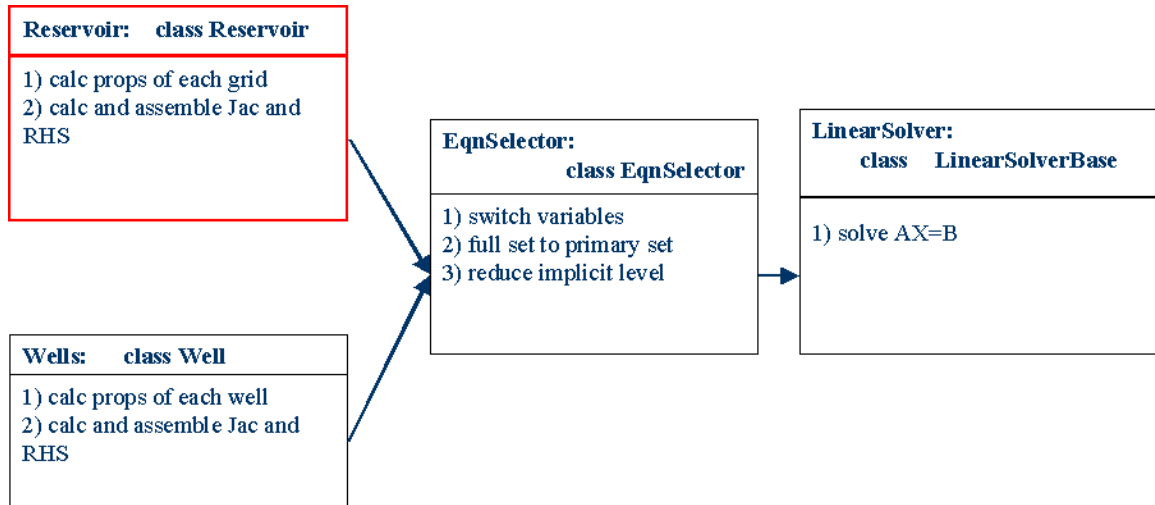


**Figure 6-7** Domain level system model

It has been mentioned earlier that the jacobian matrices are calculated separately for the reservoir part and for the well part. Figure 6.8 shows the system model for each of the reservoir part. From Figure 6.8, we can see that, each reservoir includes a grid and a formulation; grid part generates the grid information and passes it to the formulation part. The formulation part calculates the gridblock properties and builds the reservoir part of the jacobian matrix and the RHS. In GPRS, the grid information is either internally generated (currently only for Cartesian grid), or read in from the output of a gridding software. Three modifications are required to the existing reservoir level system module as shown in red (circles).

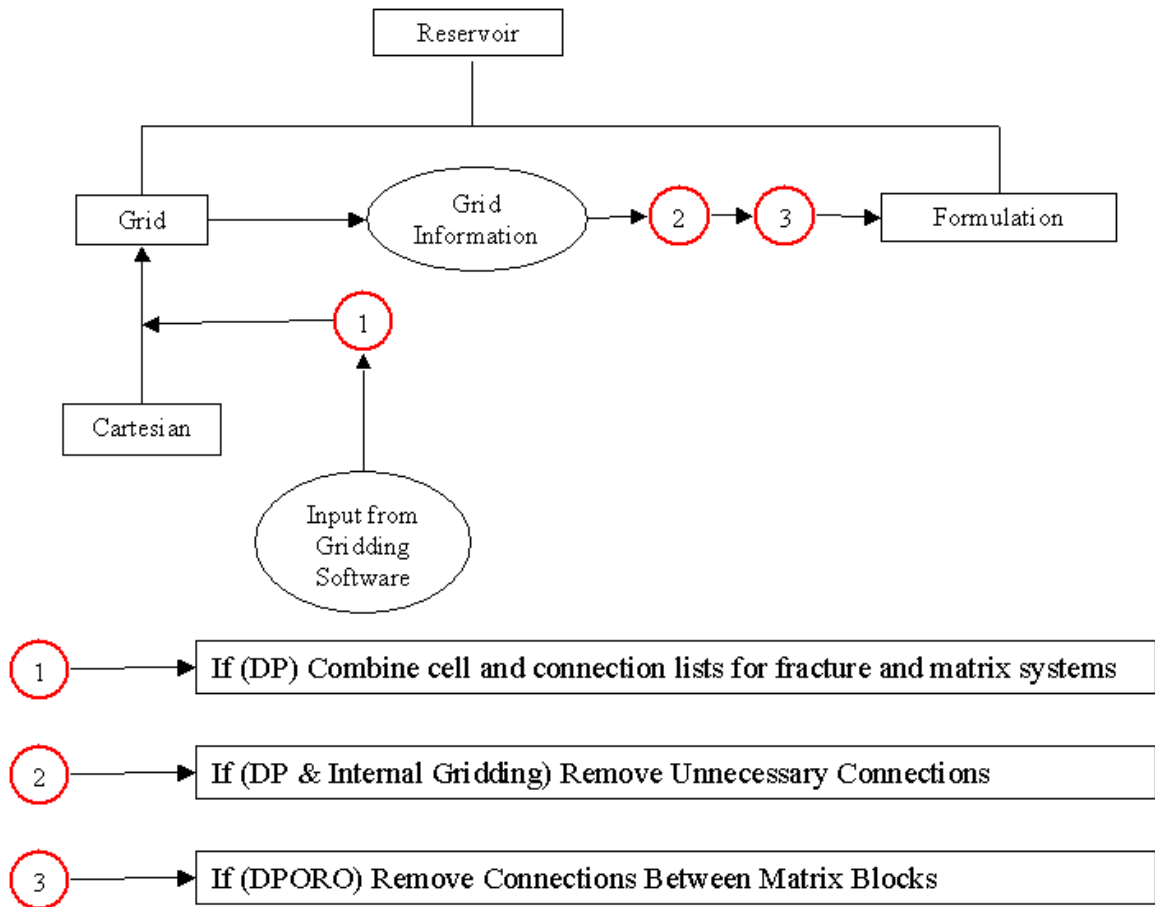


**Figure 6-8** Reservoir level system model (modified)

At 1, since we have two cell and two connection lists for a NFR model, both need to be combined into one each. The cell and connection numbers would be the same in both sets of lists, but the properties associated with the same cell (volume, porosity) and same connection (transmissibility constant) would be different for the two sets. Thus, before combination, the cell numbers and connection numbers in the fracture lists have to be increased by  $N$  ( $2N = \text{total grids}$ ), keeping properties same.

At 2, since the internal gridding will create connections between the  $NZ/2$  and  $NZ/2 + 1$  layers, these have to be removed as they are not physical for a dual porosity/ dual permeability model.

At 3, if dual porosity instead of dual permeability is used, the connections between the matrix gridblocks have to be removed.

Figure 6.9 shows the formulation system model. The entire reservoir related calculations are carried out here. The calculations are organized using five mathematical modules: one for rock, one for fluid, one for rock/fluid, one for phase mobility and the last one for flow equations. Each of these classes starts with the header '*mth*', as seen in Figure 6-9. Most of the gridblock properties are calculated in the first four modules, and the reservoir part of the jacobian matrix and the RHS are calculated and assembled in the last module. If necessary, each module can have multiple subclasses for different models. For example, the fluid part has a black-oil and a compositional module. If a module has connections to the physical world, such as the rock module, it will have a pointer to the corresponding physical object. For example, the **Rock** class and the **BOFluid** class seen in Figure 6-9 are classes representing physical properties of the reservoir rock and black oil fluids. All of the mathematical modules are organized in a multi-level inheritance structure, they all share the same public interface (methods), and dynamic binding is used to determine the actual objects and methods required during a run.

The last row (red boxes with spotted background) of Figure 6-9 shows the modifications required to implement the dual porosity/dual permeability model. The changes required in formulation as discussed above are captured through new classes inherited from the **mthFlowEquation** module. This is also shown in Figure 6-9 and 6-10. In addition to this, there are four major modifications required to complete the implementation. Since a dual porosity reservoir contains two types of rock (matrix and fracture) as compared to one for single porosity reservoirs, the physical Rock class has to be modified. This is done by inheriting a new class **DPRock** from the **Rock** class. Similarly two sets of relative permeability and capillary pressure curves are required for dual porosity systems, and this is implemented by inheriting a new class **DPRockFluid** from the **RockFluid** Class. And as we saw before changes in the grid representing the reservoir are also needed, which is done through the **DPGrid** class inherited from the **Grid** class. The final modification required is to implement the **DPSigma** class that incorporates the two shape factors required for the proposed dual porosity model.

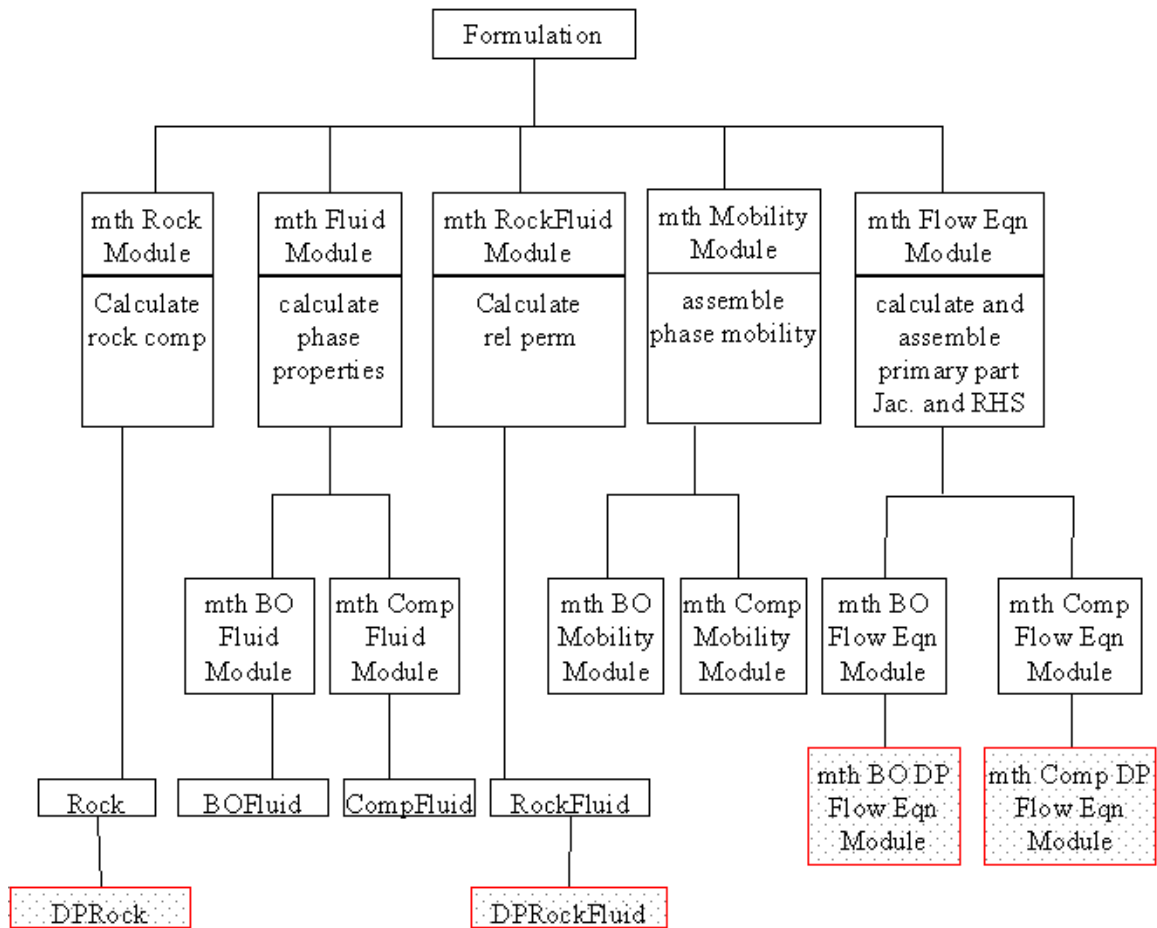


Figure 6-9 Modifies formulation level system model

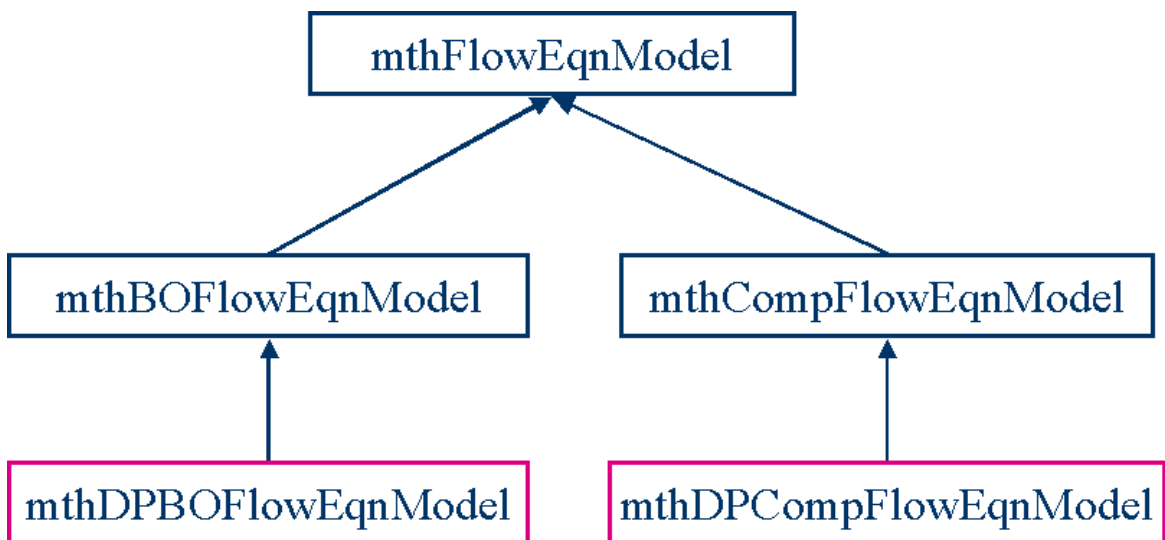


Figure 6-10 Inheritance structure for the flow equation modules

To complete the implementation, the only change that is required in a client class is in the **Reservoir** class, in which switching statements are required based on whether a run is a single porosity or dual porosity run. The following code showing the changes in **Reservoir** class to implement the new **DPGrid** class exemplifies the process:

```
class Reservoir::Reservoir()      //old code
{
    // other code
    mGrid = new Grid(fio);
    // other code
}

class Reservoir::Reservoir()      //new code
{
    // other code
    if(Dual Porosity)
        mGrid = new DPGrid(fio);
    else
        mGrid = new Grid(fio);
    // other code
}
```

Also, as mentioned before, a few changes are required in the **Equation Selector** class and the **Linear Solver** class. These are again implemented by inheriting new classes from these and making the necessary modifications to the new classes.

The current version of the dual porosity/dual permeability implementation in GPRS does not incorporate all of the above modifications. In particular, only the black oil multipoint flux formulation has been implemented. Further, variable switching and reduction in implicit level are not yet operational, i.e., only Type A variables in fully implicit mode can be used. Lastly, only a few of the existing linear solver classes have been modified to handle dual porosity/dual permeability simulation.

### 6.3. Validation of the Standard Model

The dual porosity/dual permeability implementation in GPRS is validated against the standard dual porosity/dual permeability model in ECLIPSE 100. It should be noted that the standard model of ECLIPSE 100 is given by the black oil version of Equations 2.26 and 2.27 and can accommodate only a pseudo-steady state shape factor (Eclipse 100 Technical Description, 2000). The test case used is an oil-water system similar to that

given by Kazemi et al. (1976) and is shown in Figure 6-11. The model is a quarter five-spot pattern with an injector in one corner and a producer in the opposite corner. Both the wells are under rate control. The relevant properties of the system are given below:

Dimensions	8x8x2	DX, DY, DZ	75, 75, 30 ft
Km, Kf	1md, 50d	$\phi_m, \phi_f$	19%, 1%
Rel Perm, Pc	Corey Type	Rel Perm, Pc Frac	X Type
Matrix Size	10x10x30 ft	Sigma	0.08 (Kazemi et al.)

**Table 6-1** Properties of the test case reservoir

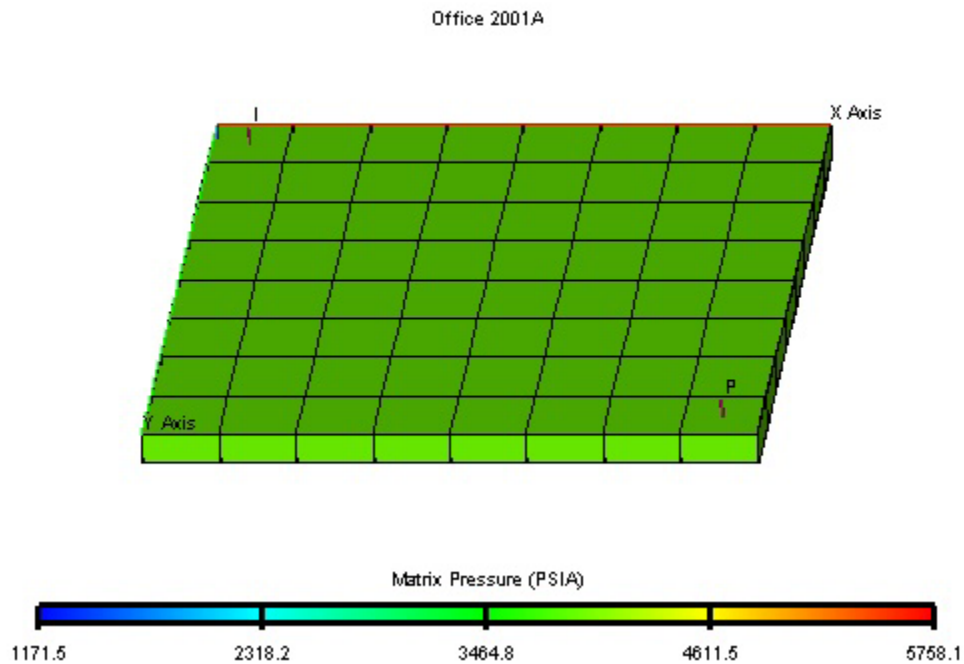


**Figure 6-11** Quarter five-spot test case

Simulation was run for 1100 days. A comparison of the producer well block pressure and water cut obtained from GPRS and ECLISPE are shown in Figures 6-12 and 6-13. Both plots show excellent agreement of GPRS and ECLISPE results, validating the implementation.

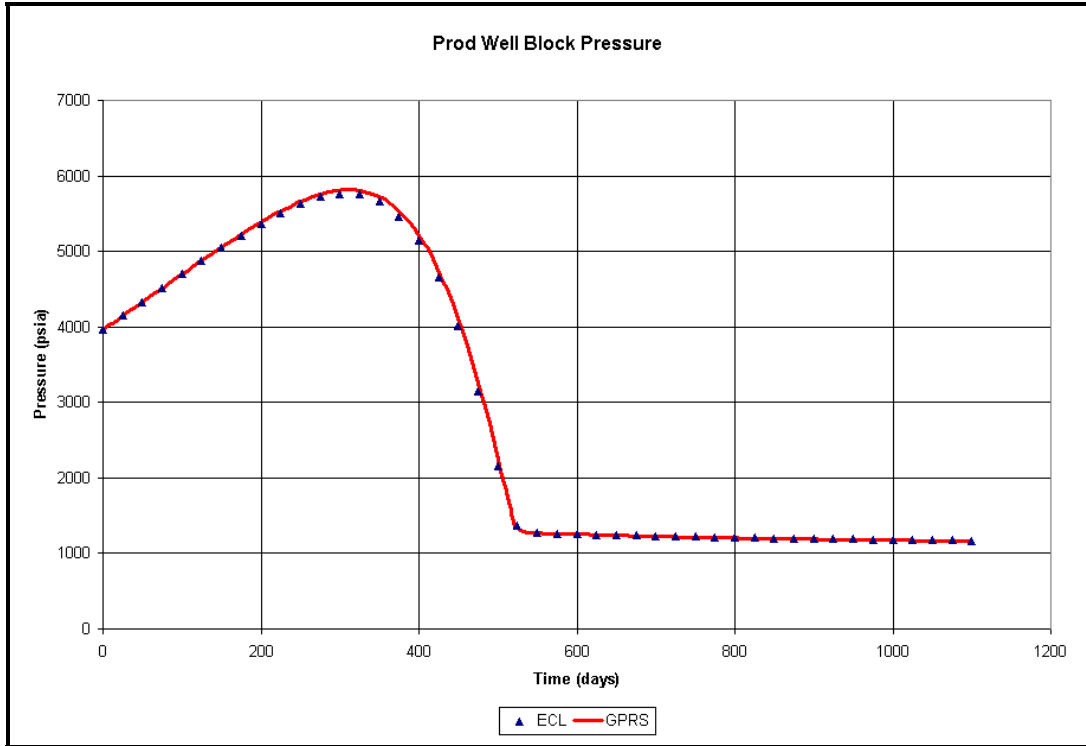


Figure 6-12 Producer well block pressure vs. time

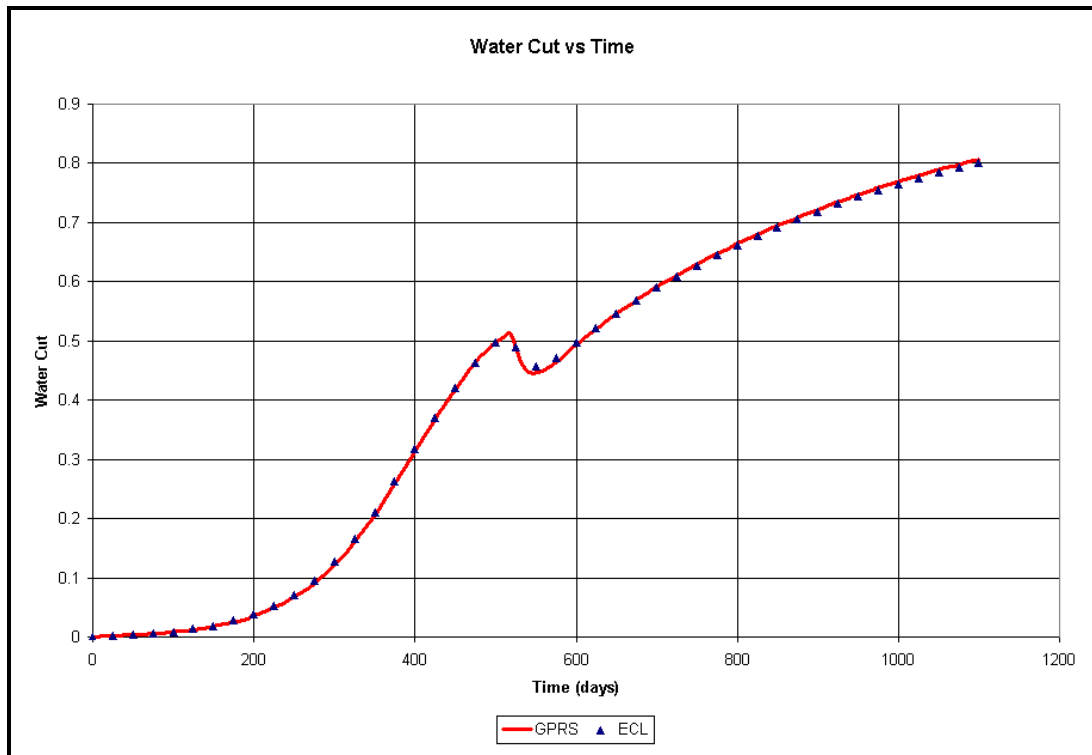


Figure 6-13 Producer water cut vs. time

## Chapter 7

### 7 Conclusions and Future Work

Through this work, an attempt has been made to improve our understanding of the flow behavior of naturally fractured reservoirs. The results derived and insights gained help us to draw a few significant conclusions.

Firstly, it is seen that although the form of the existing transfer function is correct for single-phase flow, most of the existing shape factors are only valid for parallelepiped matrix blocks and pseudo-steady state flow. It is shown that this might not always be a good approximation for certain NFRs where transient and non-orthogonality effects are dominant. The effect of transient flow and non-orthogonality of the fracture system is verified mathematically. It is seen that a time variant shape factor is required to model transient flow. It is also acknowledged that the rate of mass transfer can vary quite significantly as a function of the non-orthogonality of the fracture system. With these insights, a general numerical technique to calculate the shape factor for any arbitrary shape of the matrix (i.e. non-orthogonal fractures) is proposed. This technique also accounts for both transient and pseudo-steady state pressure behavior. The results were verified against fine-grid single porosity models and were found to be in excellent agreement.

Secondly, mechanisms of two-phase mass transfer are studied and it is shown that fluid expansion and imbibition are the main driving forces governing dual porosity mass transfer. However, the existing multiphase transfer function is a direct generalization of the single-phase transfer function, and since the only mechanism governing single-phase flow is fluid expansion, this generalization is not accurate. With this insight, a modified transfer function is derived that accurately accounts for fluid expansion and imbibition. The new transfer function separates the effects of fluid expansion and imbibition into two different terms. It is seen that the term for fluid expansion is the same as the existing

transfer function, and the shape factor derived for fluid expansion is the same as that obtained for single-phase flow. The term for imbibition requires a new shape factor and it is seen that this shape factor is a function of time. It is observed that while prediction of wetting phase imbibition is inaccurate with the existing transfer function, the new transfer function matches fine grid simulations very well, verifying its validity.

Thirdly, it is seen that the new transfer function derived for immiscible two-phase flow can be easily generalized to three-phase compositional flow. This is based on the observation that addition of a third phase does not add any new mechanisms governing dual porosity mass transfer. The effect of gravity segregation is also added by assuming that linear superposition of the three mechanisms is applicable. However, the validity of the above assumption is not verified.

With the background acquired in the course of this research the following recommendations for future work are suggested.

1. As mentioned before, the effect of transient shape factors should be significant in the analysis of well test results through numerical well testing. In order to gain a quantitative understanding of the magnitude of this effect, case studies are required.
2. Field scale simulations are required to gain a quantitative understanding of the effect of fracture non-orthogonality to production performance of NFRs.
3. The consequences of the new transfer function for multiphase flow on a field scale model should be significant but are yet to be determined.
4. A rigorous transfer function incorporating the effect of gravity segregation does not yet exist and is desirable.
5. One major assumption in existing dual porosity models is that all matrix blocks within a grid block are assumed to have the same pressure and saturation distribution. The validity of the above assumption needs to be verified, and if possible a multiple matrix block transfer function derived.
6. Extend the dual porosity/dual permeability model in GPRS to include compositional simulation, variable switching and reduction in implicit level.



## Nomenclature

$A$	Area of surface between two gridblocks, [ft <sup>2</sup> ]
$D$	Depth, [ft]
$k$	Absolute permeability, [md]
$k_{rp}$	Relative permeability of phase $p$
$L, l$	Fracture length [ft]
$n_c$	Number of components
$n_p$	Number of phases
$P_{c,p_1,p_2}$	Capillary pressure between phase $p_1$ and phase $p_2$ , [psia]
$p$	Block pressure, [psia]
$p^w$	Wellbore pressure of well $W$ , [psia]
$P$	Dimensionless pressure
$q$	Rate of mass transfer [lbm/day]
$S_p$	Saturation of phase $p$
$t$	Time [day]
$T$	Transmissibility, [md·ft]
$V$	Volume, [ft <sup>3</sup> ]
$WI^w$	Well Index of well $W$ , [md·ft]
$X_{c,p}$	Mole fraction of component $c$ in phase $p$

## Acronyms

GPRS	General Purpose Research Simulator
NFR	Naturally Fractured Reservoir
FEM	Finite Element Method
Type A	Type A variables (pressure, saturations and component mole fractions)
Type B	Type B variables (pressure, overall component densities)

## Greek

$\sigma_{PD}$	Shape Factor for pressure diffusion [1/ft <sup>2</sup> ]
$\sigma_{SD}$	Shape Factor for saturation diffusion [1/day]
$\alpha$	Angle between fractures [degrees]
$\lambda_p$	Mobility of phase $p$ , [1/cp]
$\rho_p$	Density of phase $p$ , [lbm/ft <sup>3</sup> ]
$\mu_p$	Viscosity of phase $p$ , [cp]
$\gamma$	Gravity constant
$\Phi_p$	Potential of phase $p$ , [psia]
$\phi$	Porosity

## Subscripts

$f$	Fracture
$m$	Matrix
$p$	Phase
$c$	Component
$w$	Water

## Superscripts

$n$	Time level $n$
$n + 1$	Time level $n + 1$
$W$	Well

## References

1. Aziz, K., Aug. 2001, "Fundamentals of Reservoir Simulation", Course notes for PE223 at Stanford University.
2. Barenblatt, G.E., Zheltov, I.P., and Kochina, I.N., 1960, "Basic Concepts in the Theory of Homogeneous Liquids in Fissured Rocks", Journal of Applied Mathematical Mechanics (USSR).
3. Beckner, B.L., 1990, "Improved Modeling of Imbibition Matrix/Fracture Fluid Transfer in Double Porosity Simulators", PhD Dissertation at Stanford University.
4. Cao, H., Jun. 2002, "Development of Techniques for General Purpose Simulators", PhD Dissertation at Stanford University.
5. Cao, H., Jun. 2002, "General Purpose Research Simulator (GPRS) Manual", Stanford University.
6. Carslaw, H.S. and Jaeger, J.C., 1959, "Conduction of Heat in Solids", Oxford Science Publications, Oxford University Press Inc., Oxford, England.
7. Chang, M., Sep. 1993, "Deriving the Shape Factor of a Fractured Rock Matrix", Technical Report NIPER-696 (DE93000170), NIPER, Bartlesville OK.
8. CMG, 2002, "IMEX User's Guide, Version 2002", Computer Modeling Group Ltd.
9. Coats, K.H., Feb. 1989, "Implicit Compositional Simulation of Single-Porosity and Dual Porosity Reservoirs", paper SPE 18427 in proceedings of the SPE Symposium on Reservoir Simulation, Houston, TX.
10. Crank, J., 1975, "The Mathematics of Diffusion", 2nd Ed., Clarendon Press, Oxford.
11. Deitel, H.M., Deitel, P.J, 1998, "C++ How to Program, 2<sup>nd</sup> Edition", Prentice Hall Ltd.
12. Fung, L.S.K., Apr. 1993, "Numerical Simulation of Naturally Fractured Reservoirs", presented at the SPE Middle East Oil Technical Conference, Bahrain.
13. GeoQuest, 2000, "Eclipse 100 Technical Description 2000A", GeoQuest, Schlumberger.
14. German, E.R., Dec. 2002, "Water Infiltration in Fractured Porous Media: In-situ Imaging, Analytical Model, and Numerical Study", PhD Dissertation at Stanford University.

15. Gilman, J.R. and Kazemi, H., Aug 1983, "Improvements in Simulation of Naturally Fractured Reservoirs", published in SPEJ.
16. Gilman, J.R., July 1986, "An Efficient Finite-Difference Method for Simulating Phase Segregation in Matrix Blocks in Double-Porosity Reservoirs", published in SPE RE.
17. He, N., Lee, S.H. et al, Mar. 2001, "Combination of Analytical, Numerical and Geostatistical Methods to Model Naturally Fractured Reservoirs", SPE 68832 presented at the SPE Western Regional Meeting held in Bakersfield, CA.
18. Kazemi, H. and Merrill, L.S., Jun. 1979, "Numerical Simulation of Water Imbibition in Fractured Cores", published in SPEJ.
19. Kazemi, H., Merrill, L., Porterfield, K. and Zeman, P., Dec. 1976, "Numerical Simulation of Water-Oil Flow in Naturally Fractured Reservoirs", published in SPEJ.
20. Landmark, Jun. 2001, "VIP Executive Technical Reference", Landmark Halliburton Co.
21. Lim, K.T. and Aziz, K., 1995, "Matrix-Fracture Transfer Shape Factors for Dual Porosity Simulators", Journal of Petroleum Science and Engineering.
22. Litvak, B.L., Apr. 1985, "Simulation and Characterization of Naturally Fractured Reservoirs", paper presented at the Reservoir Characterization Technical Conference, Dallas, TX.
23. MathWorks, 1996, "Matlab PDE Toolbox User's Guide", The MathWorks Inc.
24. Ordonez, A., Penuela, G. et al., Dec. 2001, "Recent Advances in Naturally Fractured Reservoir Modeling", published in CT&F, Vol. 2.
25. Pruess, I., and Narasimhan, T.X., Feb. 1985, "A Practical Method for Modeling Fluid and Heat Flow in Fractured Porous Media", published in SPEJ.
26. Rossen, R.H. and Shen, E.I., Sept. 1987, "Simulation of Gas/Oil Drainage and Water/Oil Imbibition in Naturally Fractured Reservoirs ", paper SPE 16982 presented at the 1987 SPE Annual Technical Conference and Exhibition, Dallas. TX.
27. Saidi, A.M., Nov. 1983, "Simulation of Naturally Fractured Reservoirs", paper SPE 12270 presented at the Seventh SPE Symposium on Reservoir Simulation held in San Francisco, CA.
28. Shaqfeh, E.S.G, Jan. 2001, "Mathematical and Computational Methods in Engineering", Course Notes for ME200B at Stanford University.

29. Sonier, F., Souillard, P. and Blaskovich, F.T., Oct. 1986, "Numerical Simulation of Naturally Fractured Reservoirs", paper SPE 15627 presented at, the 1986 SPE Annual Technical Conference and Exhibition, New Orleans, LA.
30. Spiegel, M.R., Liu, J., 1999, "Mathematical Handbook of Formulas and Tables, 2<sup>nd</sup> Edition", McGraw Hill Ltd.
31. Thomas, L.K., Dixon, T.N. and Pierson, R.G., Aug. 1983, "Fractured Reservoir Simulation", published in SPEJ.
32. Van Golf-Racht, T. D., May 1982, "Fundamentals of Fractured Reservoir Engineering", Elsevier Science Ltd.
33. Warren, J.E. and Root, P.J., Sept. 1963, "The Behavior of Naturally Fractured Reservoirs", published in SPEJ.
34. Wu, Y.S. and Pruess, K., Apr. 1986, "A Multiple-Porosity Method for Simulation of Naturally Fractured Petroleum Reservoirs", paper SPE 15129 presented at the 56th California Regional Meeting held in Oakland, CA.
35. [www.fracturedreservoirs.com](http://www.fracturedreservoirs.com), Aug. 2000, "Circle Ridge Fractured Reservoir Project", Golder Associates, Redmond, WA.

# Appendix A

## A. Shape Factor Software

The software to numerically calculate the shape factor for any arbitrary shape of the matrix block has been designed in Matlab using the PDE Toolbox. The script to run is *'main.m'*. It takes a data file as input that among other things specifies the shape and size of the matrix. The shape is given in the form of coordinates of the corners (x,y) of the polygon defining the matrix shape. An example data file is as shown below.

```
POROSITY           // Percent
5
VISCOSITY          // cp
1
COMPRESSIBILITY // 1/psi
1e-4
PERMEABILITY       // md
0.1
TOTAL_TIME         // days
50
TIME_STEP          // days
0.1
MATRIX_SIDES       // number of sides of the matrix
4
COORDINATES        // coordinates of the corners, ft
0.0  0.0
10.0 0.0
10.0 10.0
0.0  10.0
```

The software generates the FEM grid automatically, but gives the user capability to refine the grid if necessary. Further, the pressure derivative calculated might not be smooth always, which can lead to oscillations in the value of the shape factor calculated. This is seen especially when pseudo-steady state is reached. The user can increase the degree of smoothness of the derivative if necessary. Although this reduces the oscillations, it can make the shape factor obtained less accurate.

## **Appendix B**

### **B. GPRS Dual Porosity Model**

A few changes are required in the standard Reservoir Input file to be used for dual porosity/dual permeability simulation. These changes are incorporated as new keywords.

#### **DUALPORO**

This keyword is used to specify a dual porosity run.

#### **DUALPERM**

This keyword is used to specify a dual permeability run.

#### **ROCKFLUID\_DATA**

This is an existing keyword, but is now used only to input the relative permeability and capillary pressure tables of the matrix system.

#### **ROCKFLUID\_DATA\_FRAC**

This keyword is used to input the relative permeability and capillary pressure tables of the fracture system.

#### **ROCK\_DATA**

This is an existing keyword, but is now used only to input rock properties (compressibility and reference pressure) of the matrix system.

#### **ROCK\_DATA\_FRAC**

This keyword is used to input rock properties (compressibility and reference pressure) of the fracture system.

For a dual porosity/dual permeability run, the number of grid layers in the Z direction has to be even. The top half layers are given the properties of the matrix system and the bottom half the properties of the fracture system.

The two shape factors are input through a file '*sigma.in*'. Two keywords are present in this file.

### **SIGMA\_PD**

This keyword is used to input the shape factor for pressure diffusion,  $\sigma_{PD}$ . It is input in the form of a table, the first column being time (days), and the second column being the shape factor (1/ft<sup>2</sup>).

### **SIGMA\_SD**

This keyword is used to input the shape factor for saturation diffusion,  $\sigma_{SD}$ . The two coefficients present in the definition of  $\sigma_{SD}$  (Equation 4.61), i.e.,  $a$  and  $m$  are input through this keyword.